# STUDY OF FLOW FIELDS IN THE TRANSITIONAL REGIME AND THEIR EFFECTS UPON AERONOMY MEASUREMENTS

FINAL REPORT

for

LOW-ALTITUDE SATELLITE INTERACTION PROBLEM INVESTIGATION STUDY

Contract No. NAS5-11016



Prepared by

RCA Astro-Electronics Division
Princeton, New Jersey

for

Goddard Space Flight Center
National Aeronautics and Space Administration
Greenbelt, Maryland



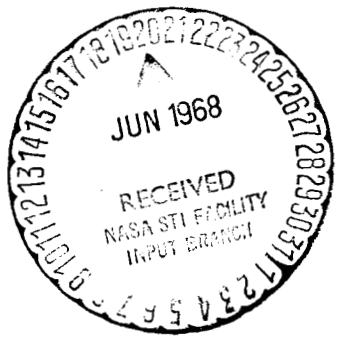


AED R-3288

Issued: May 17, 1968

# STUDY OF FLOW FIELDS IN THE TRANSITIONAL REGIME AND THEIR EFFECTS UPON AERONOMY MEASUREMENTS

FINAL REPORT

for

LOW-ALTITUDE SATELLITE
INTERACTION PROBLEM INVESTIGATION
STUDY

Contract No. NAS5-11016

Goddard Space Flight Center

Contracting Officer: J.L. Turner
Technical Monitor: C.R. Reber

Prepared by

RCA Astro-Electronics Division
Princeton, New Jersey
Project Manager: L.E. Golden

for

Goddard Space Flight Center
National Aeronautics and Space Administration
Greenbelt, Maryland

# PREFACE

This is the final report on the Low-Altitude Satellite Interaction Problem Investigation Study. The study was conducted by the Astro-Electronics Division of RCA for the National Aeronautics and Space Administration under Contract No. NAS5-11016. Work on the study was accomplished during the period from March 31, 1967 through January 31, 1968.

# SUMMARY

Many important phenomena that affect the structure of the upper atmosphere occur in the altitude range of 100 to 150 kilometers. The need for aeronomic measurements at this altitude is well known. A rocket or satellite vehicle of ordinary size (on the order of meters) moving through this altitude range produces an interaction with the gas in the vicinity of the vehicle. This interaction cannot be described by either the free-molecular or continuum-fluid mechanical theory, and is generally considered to be in the "transition" regime. In order to enable interpretation of measurements made on or near the vehicle surface, it is necessary to have a theoretical means of determining how the state of the gas deviates from its ambient condition during such an interaction. The objective of the present study is to provide a means for computing the effect of the vehicle on the gas in its vicinity for flows in the transition regime, and to obtain preliminary information on the trends and magnitudes of the parameters affecting data interpretation.

This report describes two specific methods for calculating the properties of these fluid flow fields. Also presented are the results of such calculations for certain ranges of flow parameters useful in illustrating the effect of the resulting flow field on fluid measurements performed during the flight of aeronomical vehicles. The main effort in the calculations ranges over Knudsen numbers* from 0.3 to 300 and vehicle velocities in excess of three times the thermal speed of the gas (speed ratio $> 3$). The specific cases treated are the two-dimensional and axi-symmetric flow field for a binary gas mixture.

A computer program based on a Monte Carlo procedure developed by G. A. Bird** and extended to gas mixtures was employed to compute the flow field around a sphere and around an infinite cylinder with axis transverse to the flow. The program is operational over a wide range of parameters, including a range of Knudsen numbers from about 0.1 to 100. It is susceptible to further generalization and extension.

Part of the study was devoted to the performance of perturbation calculations for large Knudsen numbers, using a linearized and modeled collision term. These calculations were intended primarily for the determination of trends and for additional checks on the Monte Carlo procedure.

*Ratio of mean free path to body size.

**Professor of Aeronautics, University of Sydney, Sydney, Australia.

The results show that there is a significant increase in the flux to the body in the vicinity of the stagnation point. The total stagnation-point flux in the Knudsen-number range of 1 to 10 is from 8 percent to 65 percent above the free-stream value. The perturbation theory suggests that the first measurable deviations from free-molecular theory may occur at Knudsen numbers in excess of 100, and thus at altitudes above 150 kilometers. In addition to the increase in total flux, there is a very pronounced enrichment of the heavy specie (for a binary gas mixture) in the vicinity of the stagnation point. This enrichment, if not included in the data-reduction process, could lead to a gross overestimate of the relative abundance of heavy species in the ambient atmosphere.

The present study has demonstrated the feasibility of determining the effects of a moving vehicle on the gas in its vicinity (in the transition regime), and has shown these effects to be an important part of the data interpretation problem. Much work remains to be done in increasing the sophistication of the model problem and extending it into more realistic geometries. Additional computations are needed in order to determine more fully the effects of the relevant parameters. Increased sophistication of the program and improved understanding of the results should provide guidelines useful in the design of aeronomy experiments and the necessary tools for the analysis or interpretation of flight data.

# TABLE OF CONTENTS

# LIST OF ILLUSTRATIONS

# LIST OF TABLES

# SECTION I
# INTRODUCTION

For more than twenty years, ballistic rocket flights have been gathering data on the upper atmosphere at altitudes above 25 or 30 kilometers. Such flights have ranged to altitudes of 300 kilometers and more. High-level balloons have also contributed to knowledge of the properties of the upper atmosphere. Similarly, with the advent of orbital flight, measurements have been made on the properties of the residual atmosphere at very high altitudes, generally above 300 kilometers. Thus, in varying degrees of detail, measurements have been made over the entire altitude range of the atmosphere. These measurements have led to a greater understanding of the physics of near-earth space. Among the most significant contributions are the proof of the existence of the Van Allen belt and data on the gross morphology of the magnetosphere.

The wealth of information that has been gathered on the atmosphere as a whole produces a reasonably coherent picture of the atmosphere; however, the need for more information on certain discrete altitude belts is felt to be quite critical. One such belt ranges from about 90 kilometers to as high as 200 kilometers, but the 30-kilometer spread on either side of the 120-kilometer level is of special interest.

Below 90 kilometers, the atmosphere is essentially hydrostatic and is homogeneously mixed. For this region, the mechanisms that control the overall behavior, such as the equilibrium values of state parameters, are reasonably well understood. Although many secondary features in the regions just below 90 kilometers are obscure, the existing theoretical framework covers the grosser features quite well. For example, the details of the mechanism of the formation of the D-layer are still rather obscure, but the reasons for the general behavior of the mesospheric temperature profile seems to be reasonably well understood.

Well above 90 kilometers, a diffusive rather than a hydrostatic equilibrium is known to prevail. Here, the word equilibrium must be understood to connote not a true equilibrium but rather mean values within an as yet poorly understood dynamical framework. The equilibrium of the gross values of the state parameters (such as composition profile) are brought about by countervailing diffusion processes. The

intervening altitude belt, in which the change is from a substantially hydrostatic to an essentially diffusive equilibrium, is understood, but in somewhat less simple terms. Such a region can be thought of as a bounding region, the data from which can be used as a boundary condition for the altitude region above. The lack of knowledge of these so-called boundary conditions contributes in some measure to the lapses in understanding of the equilibrium state in the upper altitudes (greater than 200 kilometers). Among the physical variables comprising these boundary conditions are the temperature, the partial densities, and partial fluxes. For example, some of the constituents found in the higher altitudes are known to be generated at lower altitudes as well as in the altitude interval in question, and to be diffused upwards. Thus, the altitude belt from 90 to 150 kilometers is very important for the aeronomist. As more data are gathered from the higher altitudes, knowledge of the state of this region is of increasing significance.

Part of the data from this altitude interval has been obtained by instrument packages on rockets flown through the interval. However, the need for a synoptic view, which really cannot be obtained by rocket flights, is taking on greater importance. This requirement suggests than an instrument package be carried on a satellite whose orbit, at least in part, traverses the altitude region of interest.

The flow fields that develop in the vicinity of a moving vehicle cause the values of state variables characterizing the atmosphere at the precise instrument position on the vehicle to be different from the values of the same variables for the undisturbed ambient. The measurements of the state variables can be referred to their free-stream or ambient values only by knowing the effect of the flow field on these variables in the vicinity of the instrument. The determination of these flow fields, for useful ranges of parameters, constitutes the effort described in this report.

For the altitude belt in question, a relatively unique flow regime develops. This is the so-called transitional flow regime; it is most appropriately characterized by the ratio of the mean free path between collisions of gas particles to the typical body dimension. This parameter, referred to as the Knudsen number (designated Kn), has a value on the order of unity for the altitude region of interest.

Two methods of solution are examined in this report: (1) A Monte Carlo procedure and (2) a perturbation procedure. A great portion of the effort during this program involved a determination of the suitability of these two methods for solving the appropriate flow problem. In the case of the perturbation procedure, the basic theory was reasonably well understood. However, its applicability to the evaluation of so-called point parameters,* such as local number flux, was by no means clear. An investigation was conducted to determine the utility of this procedure for such calculations. In the case of the Monte Carlo procedure, the same question was at issue; namely,

*As opposed to integral parameters, such as drag.

was this a sufficiently useful method to solve, with reasonable accuracy, the flow problem at hand.

The results of the work have clearly shown that the latter method is very useful. Appropriate quantities are calculable for ranges of parameters (such as shape, Knudsen number, and Mach number) deemed useful for measurement interpretation. Typical results of these calculations are presented in this report.

# SECTION II
# THEORETICAL FOUNDATION

From the most fundamental point of view, the study of fluid motions is an aspect of the so-called many-body problem. Here, a group of N molecules may be represented by an ensemble of dynamically similar systems. The basic starting point in the analysis of such a problem is the Liouville theorem, which provides the fundamental kinetic equation. However, because it includes all higher order collisions, this approach is somewhat more general than is required for motions in gases and, in particular, for motions in so-called rarefied gases. The level of complexity required is provided by the so-called one-particle distribution function. The Boltzmann equation, which can be obtained from the Liouville Theorem, can provide the appropriate distribution function as a solution with an adequate level of information. The distribution function is the fundamental physical variable involved. It describes the distribution in velocity and configuration space of the gas molecules of the fluid system. Its velocity moments provide the flow variables desired.

From a simple physical point of view, the collisions, or more properly the encounters, between the molecules constituting the gas are the fundamental dynamical process. This is so because there are no external forces (other than the presence of solid boundaries) imposed on the fluid. The collisions "connect" one part of the gas with any other part. The presence of a body, and the particular boundary conditions it provides, can influence the flow field in its vicinity through such collisions.

Since the object of the present investigation is a so-called rarefied gas flow, the Boltzmann equation or its modeled equivalent will constitute an appropriate starting point of the analysis.

In terms of the average mean free path between collisions, gaseous flow fields can be divided into three general categories. For mean free paths very much shorter than any typical dimension of the body, the so-called continuum regime applies. When, on the other hand, the mean free path is very much larger than any other critical dimension, the so-called free flow analysis applies. Obviously, here, collisions between gas particles play only a vestigal part in their dynamics. Lastly, when the length of the mean free path is of the order of a typical body dimension, the transitional flow regime is applicable. This latter regime is the flow regime of concern in this report.

Fundamentally, the Boltzmann equation governs all three regions, however, the particular methods of solution are profoundly affected by the size of the Knudsen number. For the transitional flow regime, the Knudsen number is of order unity.

The Boltzmann equation for a gas mixture is given as:

$$\frac{\partial f_i}{\partial t} + v_i \cdot \frac{\partial f_i}{\partial r_i} + F_i \cdot \frac{\partial f_i}{\partial v_i} = \sum_j \iiiint \left( f'_i f'_j - f_i f_j \right) k_{ij} \, dk_{ij} \, dv_j \qquad (1)$$

where

$f_i (r_i, v_i t)$ is the distribution function of the $i^{th}$ species,

$t$ is the time,

$v_i$ is the instantaneous velocity,

$r_i$ is the position coordinate,

(') is the superscript prime (implies post-collision quantities)

$k_{ij}$ is the encounter variable, and

$F_i$ is the external force on the $i^{th}$ species.

The solution of Equation 1 describes the temporal and spatial evolution of the distribution function of the $i^{th}$ gas component. For a $j^-$ component gas mixture, there are j such equations which are coupled by the so-called collision term on the right-hand side. The product $f_i (r_i, v_i t)$ dr dv dt can be interpreted as the probability of finding, a particle in a region of configuration space between $\vec{r}$ and $\vec{r} + \vec{dr}$ and simultaneously in a region of velocity space between $\vec{v}$ and $\vec{v} + \vec{dv}$, in a time interval between t and t + dt. It can also be defined as the number of particles found in the above intervals of time, configuration and velocity space. Such distinctions in definition arise as a result of the particular choice of normalization of the function $f_i$.

Despite the complexity of Equation 1 as given (it is a non-linear, partial-differential integral equation), it lacks generality on two grounds. First, it ignores other than binary collisions; that is, molecular encounters in which more than two molecules are involved. As pointed out above, this is of no practical importance in low-density gases. The second lapse from generality is that it ignores the internal structure of the gas molecules. In gases for which the temperature is great enough so that a collision can change the internal energy configuration of a molecule, explicit recognition must be taken of this in the collision term. Collisions that change the internal energy states of gas molecules are referred to as inelastic collisions. These collisions can leave

one or both colliding molecules in an excited internal state. Some of the kinetic energy of translation exchanged between two particles, can in this case, be channeled into exciting (or de-exciting) an internal state. In such a situation, the distribution function of the $i^{th}$ species $f_i$ takes on a more restricted meaning. Here $f_i$ would have to become $f_{il}$ where the index i would refer to the particular component of the mixture and the l to the $l^{th}$ internal state of the $i^{th}$ species.

Formally, the equation would not appear different but the encounter variable $k_{ij}$ would now acquire a more complex meaning. Under these circumstances, the encounter variable must describe the dynamics of a collision in which a species i in an internal state l collides with a species k in a state m and results in an internal state l' of i and m' of k. The encounter variable for such collisions would likely assume a complex tensor character due to the fact that the results of collisions depend not only on relative distance but also on the relative angular orientation of the colliding particles. Practical effects, such as the reduction of heat transfer, occur when molecules possess internal states that can become excited. This second lack of generality can affect, in some respects, the problem at hand. In particular, such practical effects can occur when the gas molecules collide with the surface of the body. However, important information can be obtained without this level of complexity and it will not affect the particular methods of analysis applied herein.

Historically, the Boltzmann equation resisted useful solutions for many years. Work began in 1859 with the discovery by Maxwell of the form of the equilibrium distribution. Boltzmann's work in the1870's resulted in his famous H-Theorem. In 1912, Hilbert first began productive mathematical approaches to solutions for the distribution function for non-uniform, non-equilibrium situations. By 1917, following Hilbert, both Chapman and Enskog had published the first useful forms for approximate solutions to the Boltzmann equation. These methods are fundamentally similar. So useful did this latter method prove to be that for many years no further advance was made on the general solutions to the equation. In 1949, H. Grad published his 13-moment method, which allowed for solutions to various problems of a type not amenable to the method of Chapman and Enskog.

Since 1950, considerable additional progress has been made in useful formulations and solutions of the basic kinetic problem. Both of the two approaches employed in this report for solutions of the basic kinetic problem have been generated since then. One such innovation, called the Krook model, consists basically of a drastic simplification of the collision term (right-hand side of Equation 1). The analysis herein consists of a perturbation procedure applied to a linearized form of this Krook equation. The other approach models the effects of encounters on the flow by the use of a small representative group of particles. In this modelling, the effects of the collisional dynamics of about 1000 particles are tracked in a region of space surrounding the body and the results are imputed to the gas as a whole. This approach, since it involves a Monte Carlo method, is referred to as the Monte Carlo procedure.

# SECTION III
# THE MONTE CARLO PROCEDURE

"Monte Carlo" is a term referring to techniques utilizing random numbers to generate solutions from which information is deduced statistically. Because of its inherently statistical nature, kinetic theory is especially well suited to Monte Carlo treatment. A number of problems in kinetic theory have been attacked by variants of Monte Carlo techniques. The method has been applied to the determination of the equation of state[1], to a number of internal-flow, free molecular problems [2, 3], to neutron transport[4], and to other analyses. Only recently, have attempts been made to apply the method to rarefied flow problems where the Knudsen number can be of order unity.[5, 6, 7, 8]

Even in terms of this relatively restricted area of applications, there are many different Monte Carlo techniques[9].

The Monte Carlo approach ranges from being a strictly mathematical technique for evaluating the complicated multi-dimensional Boltzmann collision integral, to a complete simulation of a number of molecules with randomness introduced only in the initial conditions. In general, however, the methods can be divided into two classes. In the first class, a distribution function is first assumed and a succession of test particles is sent to interact with this distribution. The process is then repeated with the modified distribution. These methods are referred to as the "Test particle" methods. In the second class, a large number of particles are followed simultaneously, yielding to some degree a direct simulation of the processes taking place in a gas. This class of methods is referred to as "direct simulation."

In the "test particle" methods, the relationship between the method and the Boltzmann equation can be shown readily to be an iteration process on the distribution function. The collision integral is evaluated at each stage with the integrand formed from products of the previous and current iterates of the distribution function. The method can, in some sense, be considered an integral iteration technique; therefore, any questions as to convergence of the iteration scheme will apply as well to the Monte Carlo technique.

In one "direct simulation" method, random numbers are introduced only to establish the initial conditions. The remainder of the trajectories are considered deterministically, with only our lack of knowledge necessitating statistics. This direct method simulates allowable microscopic states of the gas, or in terms of kinetic theory,

members of the ensemble. The distribution among the states arising from the different initial conditions will therefore correspond to the distribution function appearing in the Bolzmann equation. If only binary collisions are allowed, the assumptions will be identical to those used in the Boltzmann equation. Generally speaking, however, such complete simulation is not feasible for problems of any complexity on even the biggest and fastest computer. One is forced, therefore, to lower the degree of simulation in a number of ways. However, as long as the samples used for the final statistical averaging are members of an ensemble that adequately models the ensemble of the true states of the gas, the solution is equivalent to that obtainable from the Boltzmann equation.

A recent development in the use of the "direct simulation" type of Monte Carlo technique by G. A. Bird[6, 7] has allowed the method to be applied successfully to problems of external flow over bodies ranging in size from much smaller than the mean free path to about ten times larger than the mean free path. The method overcomes the storage-limitation difficulties of the "direct simulation" technique by considering the N particles chosen for study not as the whole system, but only as a sample of the much larger number. Because it is to be a representative sample from the particles of the real system, the mean free path becomes uncoupled from the number N actually used on the computation and depends upon the collisions in the real gas. For steady-state flow problems, where there is constant flux of new particles entering the volume of interest, sampling over initial conditions can be avoided by averaging over a time interval once steady-state condition is reached. This technique greatly reduces the computational time.

Bird's method, in terms of its application to the problem at hand, is described more fully in succeeding sections. In this section, its general properties are given only in sufficient detail to make plausible its use as a simulation of problems describable by the Boltzmann equation.

The physical volume of interest (a finite volume of gas surrounding the body) is divided into a number of cells. These cells are populated with a certain number of particles in random positions, and with velocities chosen at random from a prescribed initial distribution. The particles are then allowed to move, and collisions are computed in each cell. The actual positions of the sample particles are disregarded since they merely represent the distribution of the much larger number of particles and since all positions within the cell are equally probable. Under these circumstances, any pair is available for collision independently of the "actual" locations of the two particles within the cell. The probability of collision is made proportional to the number of the particles in a given cell, their relative velocity and cross-section.

In this respect, the above method simulates the Boltzmann equation. Higher order collisions (i.e., three particles or more) are uncorrelated, and therefore the distribution of these ensemble members, each of which are samples of N particles out of a much larger number M, models the distribution of ensemble members, each composed of

M particles, except for the normalization factors. In addition, the method allows sampling of ensemble members in steady-state problems to be done at time intervals sufficiently long so that the streaming motion substantially replaces all particles in each cell. This longer sampling effectively produces a new "uncorrelated" ensemble member; therefore, the computing time required to obtain reasonable accuracy is reduced.

## A. SPECIFIC APPLICATION OF BIRD'S MONTE CARLO TECHNIQUE

In the technique under discussion, Bird's method [7], is extended to binary gas mixtures and modified to eliminate certain programming errors. For convenience, an outline of the basic description of Bird's method for single-specie, two-dimensional flow is given below. "Two-dimensional" means either no variation along one Cartesian coordinate, or axial symmetry.

The approach is to conduct numerical experiments with a model gas on the computer. The real gas is simulated by the order of a thousand rigid-sphere molecules which may be thought of as a representative sample of the many billions of molecules in the corresponding real gas. The positions and velocity components of the simulated molecules are stored in the computer, and typical collisions are computed among them as a time parameter is advanced. The computation of collisions starts at zero time, the molecules having been set up as a uniform stream at the required free-stream Mach number, with the thermal motion superposed. The body is inserted into this flow at zero time and the desired steady flow is obtained as the large time solution of the resulting unsteady flow.

The free-stream flow is in the positive x direction. The simulated region is bounded by the x axis as a line of symmetry and by the upstream, outer, and downstream boundaries. These boundaries must be set sufficiently far from the body to eliminate interference. The simulated region is divided into a number of cells that are sufficiently small for the change in flow properties across the cell to be small.

Figure 1a shows a side view (in a plane containing the direction of flow) of the typical cell structure for either a cylinder or a sphere. For the cylinder, the side-view plane is perpendicular to the axis of the cylinder. Figure 1b shows the cross-section in a plane perpendicular to the direction of flow. For the cylinder, the length of the cells in the direction along the cylinder axis need not be specified, because for an infinite cylinder, all properties are invariant in that direction. (This length is denoted by $\ell$ in Figure 1b.) For the sphere, the cells are annular regions; a 90-degree segment of their cross-section, in a plane perpendicular to the direction of flow, is shown in Figure 1c. In the flow around a sphere, axial symmetry exists around an axis along the direction of flow; therefore, the angular positions within the cells need not be considered.

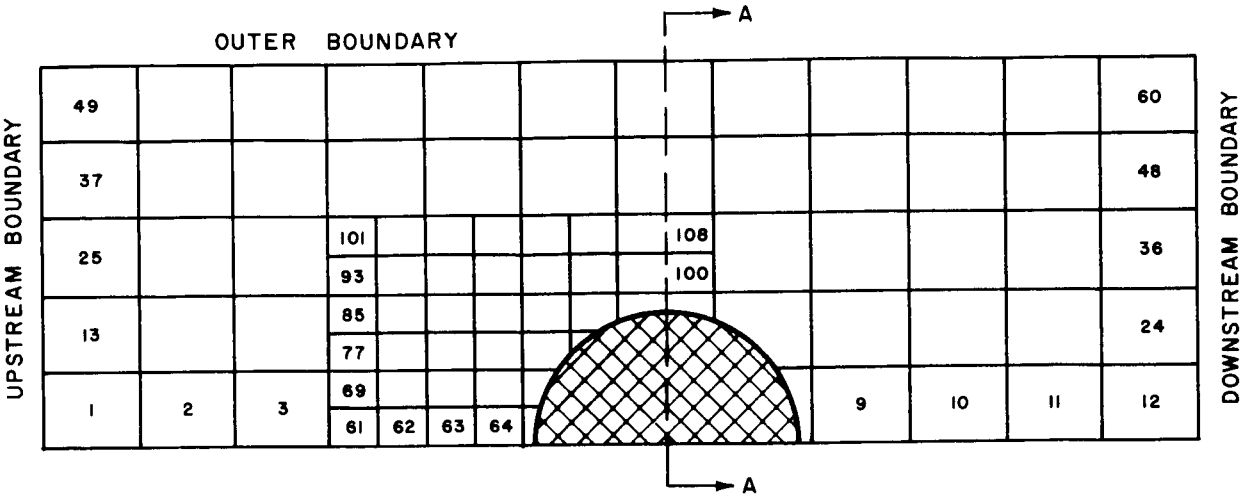


a) SIDEVIEW – CYLINDER OR SPHERE
(FLOW DIRECTION (X) IS FROM LEFT TO RIGHT)

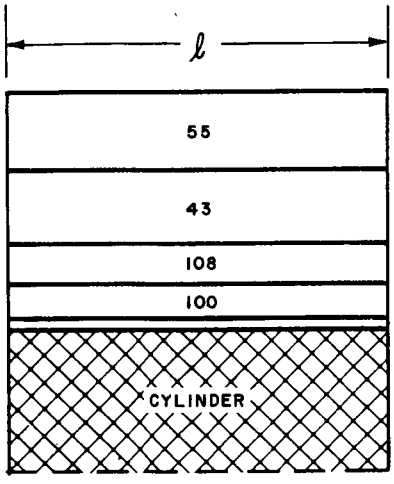


b) SECTION A-A FOR CYLINDER
($\ell$ IS AN ARBITRARY LENGTH ALONG INFINITE CYLINDER)

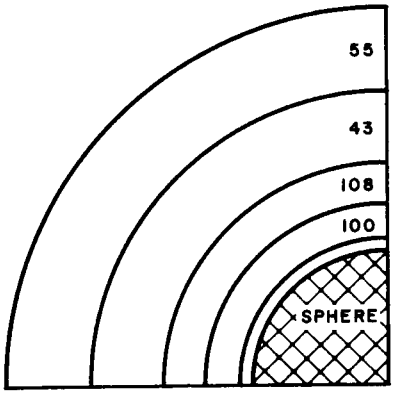


c) SECTION A-A FOR SPHERE (CELLS EXTEND 360° ALTHOUGH ONLY 90° IS SHOWN)

Figure 1. Geometry and Typical Numbering of Cells for Flow Around Cylinders and Spheres

In general, when the flow is either two-dimensional or axi-symmetric, only two position coordinates need be stored for each simulated molecule. The three velocity components are also stored and a record is kept of the molecules within each cell.

The first step is to generate the initial, or zero time, configuration of molecules. The molecules are distributed uniformly over the simulated region and the velocity components are appropriate for a gas in Maxwellian equilibrium and moving at the required Mach number.

The body is then inserted into the flow and the molecules are allowed to move and collide among themselves. The two processes are uncoupled by computing collisions appropriate for a time interval $\Delta t_m$ and then moving the molecules through distances appropriate for $\Delta t_m$ and the instantaneous velocities of the molecules. The distortion produced in the molecular paths by this approximation is small as long as $\Delta t_m$ is small compared with the mean time between collisions.

Since the change in flow properties over the width of each cell is small, the molecules in a cell at any instant may be regarded as a sample of the molecules at the location of the cell. The relative location of the various molecules within the cell can then be disregarded and the collision probability of a particular pair of molecules within the cell depends only on their relative velocity. A pair of molecules is chosen at random from those within the cell under consideration; the pair is retained or rejected in such a way that the probability of retention is proportional to the relative velocity $v_r$. When a pair is retained, a typical collision is computed between the two molecules and the new velocity components are stored in place of the old ones. The random selection of impact parameters is particularly simple for rigid-sphere molecules since all directions for the new relative velocity vector are equally probable. For each collision, the time counter for this cell is advanced by

$$\Delta t = \left(\frac{2}{N_c}\right) \times \left(\pi \sigma^2 n v_R\right)^{-1}$$

where

$N_c$ is the actual number of molecules in the cell,

$\sigma$ is the particle diameter used in the collision cross-section,

$n$ is the number density of molecules in the cell, and

$v_R$ is the relative velocity.

Collisions are computed in the cell until the time counter has advanced through $\Delta t_m$. When this procedure has been carried out for every cell, the overall time is advanced through $\Delta t_m$ and the molecules are moved through appropriate distances.

The set of molecules in each cell will change as the molecules are moved and appropriate conditions must be applied at the boundaries of the region being simulated. The upstream boundary normal to the free-stream direction is treated as a source of molecules with velocity components representative of the downstream moving molecules in the equilibrium free stream. Any molecule which moves back upstream across this boundary is regarded as being "lost" and is removed from the store. The plane of symmetry along the x axis is regarded as a specularly reflecting surface in two-dimensional flows. The outer and rear surfaces present greater difficulties. The procedure that has been developed usually introduces only a small reflected disturbance and becomes exact in free-molecule flow. A molecule is regarded as "lost" if it moves outward across the boundary, but a molecule that moves inward from the boundary during the time interval $\Delta t_m$, through a distance greater than its original distance from the boundary, is located at the new position and a similar molecule is added in the original position. The latter part of this procedure is only applied to those molecules with properties similar to the free-stream molecules. An alternative procedure is to regard the outer boundary as a specularly reflecting surface. While this would result in a larger reflected disturbance, it does permit a simple physical interpretation. Both boundary conditions produce disturbances only in a limited region, and care is taken to exclude the body from that region.

Interactions with the body are also computed. The body is assumed to have a diffusely reflecting surface with an accommodation coefficient of unity, although any other interaction model can be easily substituted. After a flow has settled down to a steady state, the momentum and energy transfer to the surface is recorded and used to compute the aerodynamic data. The time required to establish steady flow is usually assumed to be close to the time required for the free stream to travel several body dimensions. The flow field properties are also sampled in the steady flow. Instantaneous samples are recorded at appropriate time intervals and these are averaged for greater accuracy. The time interval for sampling $\Delta t_s$ is on the order of the time required for the flow to traverse one cell.

The results become progressively more accurate as the sample size is increased and the statistical scatter is reduced. An indication of the order of this scatter is given by the normal distribution result; that is, the standard deviation is equal to the reciprocal of the square root of the number in the sample. Thus 68.3 percent of the results should lie within one standard deviation, 95.5 percent within two deviations, and 99.7 percent within three deviations. Successful runs have been made with as few as six simulated molecules in each cell; the statistical fluctuations do not appear to induce instabilities in the flow.

The key to the simulation is the procedure. The molecules for a collision pair are selected according to the correct probability and then the time parameter is advanced by the appropriate amount for each collision. In this way, an appropriate set of collisions is computed for any distribution function of molecular velocities. Apart from the boundary conditions, only two approximations are made. The first is the uncoupling

of the molecular collisions and motion; this approximation becomes exact as $\Delta t_m$ tends to zero. The second is the assumption of uniform properties over the cell; this approximation also becomes exact as the cell size tends to zero.

The extension to binary gas mixtures is in principle straightforward. It consists primarily of changing all variables connected with the particles to arrays. The first member of the array denotes A particles and the second denotes B particles. The time counter is changed to an array that keeps track of AA, AB, and BB collisions separately. Although in principle this should be sufficient, the necessity of having a reasonably large sample of each specie for meaningful averaging normally precludes the possibility of obtaining solutions for large number density ratios between the two species. This problem is circumvented by always starting with the same number of A and B particles and incorporating the density ratio as a factor that accounts for the fact that B particles may be a sample of a much larger group than A particles. This factor is introduced into the collision counting process in such a way that collision probabilities are in the proper relation to each other for the true density ratio. The standard deviations for the two species, however, are based on the actual sample sizes and are therefore of the same order.

## B. CRITIQUE AND LIMITATIONS OF MONTE CARLO METHOD

There is, of course, an irreducible accuracy limitation in the method which cannot be lowered by increasing the running time. This limitation arises from the finite cell size, which because of the computer storage limitations cannot be made arbitarily small. It is difficult to place a precise value on the error arising from finite cell size; however, this error can be estimated on the basis of the solution obtained. The relative error would not be expected to exceed $\left|\frac{\nabla \phi}{\phi}\right| d$, where $\phi$ is any property of interest, $\nabla \phi$ its gradient, and d is a cell length dimension. A certain amount of difficulty may be circumvented by choosing the cell sizes so that cells in regions of high gradients are much smaller than in the rest of the flow field. Such a method has been shown to be feasible.

Another limitation and possible difficulty in the Monte Carlo method arises from the finite storage limitation of the computer. Because of this limitation, it is necessary to apply boundary conditions on the outer edges of a finite volume, when in reality they should be applied at infinity. To some extent, this problem can be investigated experimentally on the computer. The locations of the outer boundaries, and the boundary conditions themselves, can be varied to determine where the solution, at certain critical regions, becomes invariant to these changes. Such an approach is expensive in terms of computer time; therefore, only a limited amount of investigation was performed along these lines. By confining ourselves to high supersonic Mach numbers, we have reasonably solid theoretical grounds on which to estimate the range of influence of the body on the flow field. Because of the high convective speed at high Mach numbers of typical molecules compared to the thermal speed, any

disturbance is primarily convected downstream, with the lateral influence spreading at a rate that is smaller by the ratio of thermal to convective speed. The upstream and upper boundary, therefore, can be reasonably placed outside the perceptible influence of the body; the boundary conditions should cause no difficulty, as the flow is essentially free stream. On the downstream side, we can only guess at the correct boundary conditions; we can, however, guarantee that those conditions will have a small effect on the body by placing the downstream boundary sufficiently far downstream so that the convective velocity will be supersonic with respect to the body.

Of course, in using any method that incorporates the concept of random numbers, it is very difficult to be certain that no inadvertent bias is introduced in any of the sampling processes. As with any theory or experiment, a certain degree of confidence can be gained by checking for internal self-consistency and by verifying some simple known limits. Both the internal self-consistency and the ability of the method to represent an equilibrium gas were tested by running the program with the body removed. Monitoring of the number of collisions showed that the collision probabilities were being properly applied to yield agreement with the theoretical values of collision frequencies. In addition, it was shown that regardless of the initial conditions, the long time behavior was one of statistical fluctuations around a mean that was representative of the equilibrium state assumed in the free stream.

# SECTION IV

# CONNECTION OF THE PERTURBATION THEORY AND THE GENERAL THEORY

The fundamental working equation employed for the solutions to the flow problem is an amended form of the Boltzmann equation. This modification, often referred to as the Krook Model* introduces a drastically simplified form for the collision term, which is the term in the Boltzmann equation where the real analytical difficulty resides. The Krook modification of the Boltzmann equation is generally regarded as the simplest approximation that has practical merit. However, it usually requires still further simplification before it can be used. The main consequences of assuming the Krook equation are examined here.

The form for the collision term in the Krook equation is given as

$$\nu (f_o - f).$$

To be of use this term must approximate at least some of the important features of the full collision term. Introduced by this term, beyond the distribution function f, are two variables $\nu$ and $f_o$. The variable $\nu$ can be interpreted as an average collision frequency; $f_o$ is a distribution, for which the explicit velocity dependence is given. It has the form

$$f_o = \frac{n}{\left(2\pi \frac{k}{m} T\right)^{3/2}} \exp \frac{(v - u)^2}{2\frac{k}{m} T}$$

where

v is the velocity of molecules, and

k is the Boltzmann constant.

It is referred to as the local Maxwellian distribution. The velocity space dependence is that of a Maxwellian distribution. However, the component terms consisting of the number density n, the mean velocity u, the temperature T, and the mass m of the gas particle are defined as functions of position. Such terms are themselves integrals over the distribution and so the form of the term is by no means as simple as it looks.

* Bhatnager-Gross-Krook Model

However, this latter feature is a difficulty that can often be circumvented by linearization when getting down to practical cases. The form for the given distribution function $f_0$ corresponds to the notion of local thermodynamic equilibrium. Such a distribution is the one that would exist for an equilibrium situation at a point; it would be appropriate to the number density, mean velocity and temperature at that point.

The H-Theorem shows that the dynamical tendency of collisions is to restore the equilibrium state. Thus any short-lived departure from equilibrium can be "erased" by collisions. Any dynamical mechanism (e.g., insertion of a body into a gas flow and the attendant gas-body collisions) applied continuously in time can cause a steady departure from equilibrium. Simultaneously, collisions between the gas molecules themselves will likewise operate continuously to offset this departure and will tend to restore equilibrium. The actual departure of the steady-state distribution from equilibrium depends upon the magnitudes of these offsetting effects. At equilibrium, the effect of collisions is to preserve the equilibrium; therefore, any modeling of the collision term should, by definition, give rise to a zero value for the equilibrium condition. The Krook term does this. In addition, it conserves momentum and energy.

Comparison of the Krook approximation and of the full collision term suggests that the approximation was obtained by an intuitive estimate of the effects of the integrations required in the full collision term. Actually, the Krook model is reasonably consistent with the more sophisticated reasoning of Bogoluibov and others. Their reasoning is that the relaxation towards equilibrium occurs on several time scales. One of the longer epochs of the temporal evolution of the gas is the so-called hydrodynamical time scale. Such effects occur in general over a time period corresponding to an average collision time. In this sense, the Krook model is a single relaxation type of model; in particular, the Krook form causes the distribution to relax to a local equilibrium on the hydrodynamical time scale. This suggests one reason why the model works for fluid problems.

It is clear nonetheless that the justification for replacing the correct collision term by the Krook form is far from rigorous. In an attempt to bridge the analytical gap between the two forms Gross and Jackson have expanded the linearized form of the complete collision term in a series of the pre-collision and post-collision velocities. Using a finite number of terms, they show an equivalence to the Krook form.

In summary, the primary usefulness of the Krook form resides in its simplified form, which allows analytic investigation. Its practical application, although quite limited, is used in this report primarily to establish trends as the flow fields approach the free-flow regime.

Appendix I presents the details of calculations using the linearized form of the Krook equation. The theory leading to the specific equation solved in this section was developed by H. Grad[10] and applied by M. Rose[11] to the problem of transitional drag on the sphere. Rose used the method of Fourier transform suggested by Grad to

obtain a first-order solution to the basic equation. This method is quite rigorous mathematically. However, the basic equation (Krook equation with source term) is quite approximative and so the necessity for formal mathematical rigor is somewhat less stringent. As this method transforms the problem into the Fourier plane, it becomes difficult to follow what is happening to the physics. As a result, this method was dropped and a simpler method was used. The method used in Appendix I is a takeoff from a traditional technique in which a coordinate transformation is effected to make the integration of the differential equation proceed along a particle trajectory. The arithmetic operations and approximations employed using this procedure have fairly obvious physical consequences; therefore, the propriety of what such mathematical operations are doing can be evaluated immediately.

In addition, with respect to evaluation of the source function, a more realistic representation than that proposed by Rose has been developed. The solution put forth by Rose gives rise to a nulling of the effects of the zero-order perturbation (free molecule flow) for certain of the moments in a direction at 90 degrees to a free-stream flow direction. The evaluation of the source function proposed here predicts a finite zero-order perturbation for the appropriate moments for the same direction. This effect is to be expected on simple physical grounds.

The solution to the perturbation analysis given here, not only provides a somewhat simpler physical picture, but, in addition, accounts for effects that are absent in previously published work. The method can be extended to mixtures consisting of an arbitrary number of gases in a straightforward though extremely tedious way. Because the primary purpose of the perturbation calculations was only to provide subsidiary information to the main effort contained in the Monte Carlo procedure, it was felt that the magnitude of the effort required to extend the perturbation procedure to binary mixtures was not justified for the value of the results. Thus, all calculations were limited to single-specie flow.

The details of the analysis are presented in Appendix I.

# SECTION V
# DISCUSSION OF RESULTS

## A. MONTE CARLO PROCEDURE

Two programs were developed and checked. Program No. 1, for flow around an infinite cylinder with axis transverse to the flow direction, was used as a test bed for the changes necessitated by the binary mixture of gases. The debugging and testing to obtain confidence in the validity of the results with respect to the modeled physical problem were performed on this program. The details of the debugging procedure are given in Appendix I. Because of the degree of confidence in the program and the relatively short computing running times necessary (about 10 to 15 minutes per case), the cylinder program was also used for an exploratory investigation of the trends in the total number flux at the stagnation point with variation of the various parameters. To examine these trends the program was run for 12 cases (12 specific sets of parameters).

Program No. 2 for flow about a sphere has also been debugged and tested for self-consistency to obtain reasonable confidence in its validity. Because of the lower degree of familiarity with possible difficulties in this program, and the much longer computing times for accuracy similar to that obtained in Program No. 1 (about 20 to 30 minutes per case), only 3 cases are available for the sphere.

Twelve production runs of Program No. 1 were made in order to test both the range of applicability of the program and to explore the trends with variation of the basic parameters of the problem. The parameters selected were the three most important non-dimensional parameters of the problem: Knudsen number, mass ratio, and number density ratio of the two gases in the free stream. The values of parameters were chosen to give the best possible definition of trends in the results, over the widest range possible. The computer outputs contain a large amount of information on the macroscopic properties of the gases in the flow field, as well as fluxes of mass, momentum, and energy to the surface. It was decided that for the purpose at hand a useful quantity to present is the number flux to the surface. Summaries of information on the variation of total number flux, and relative flux of the two species are contained in Figures 2 through 5 and Tables 1 through 6. The curves in the figures are only illustrative of the trends; in general, they are drawn through only three calculated points, which are shown in the various figures. The value of the standard deviation is given with each point.

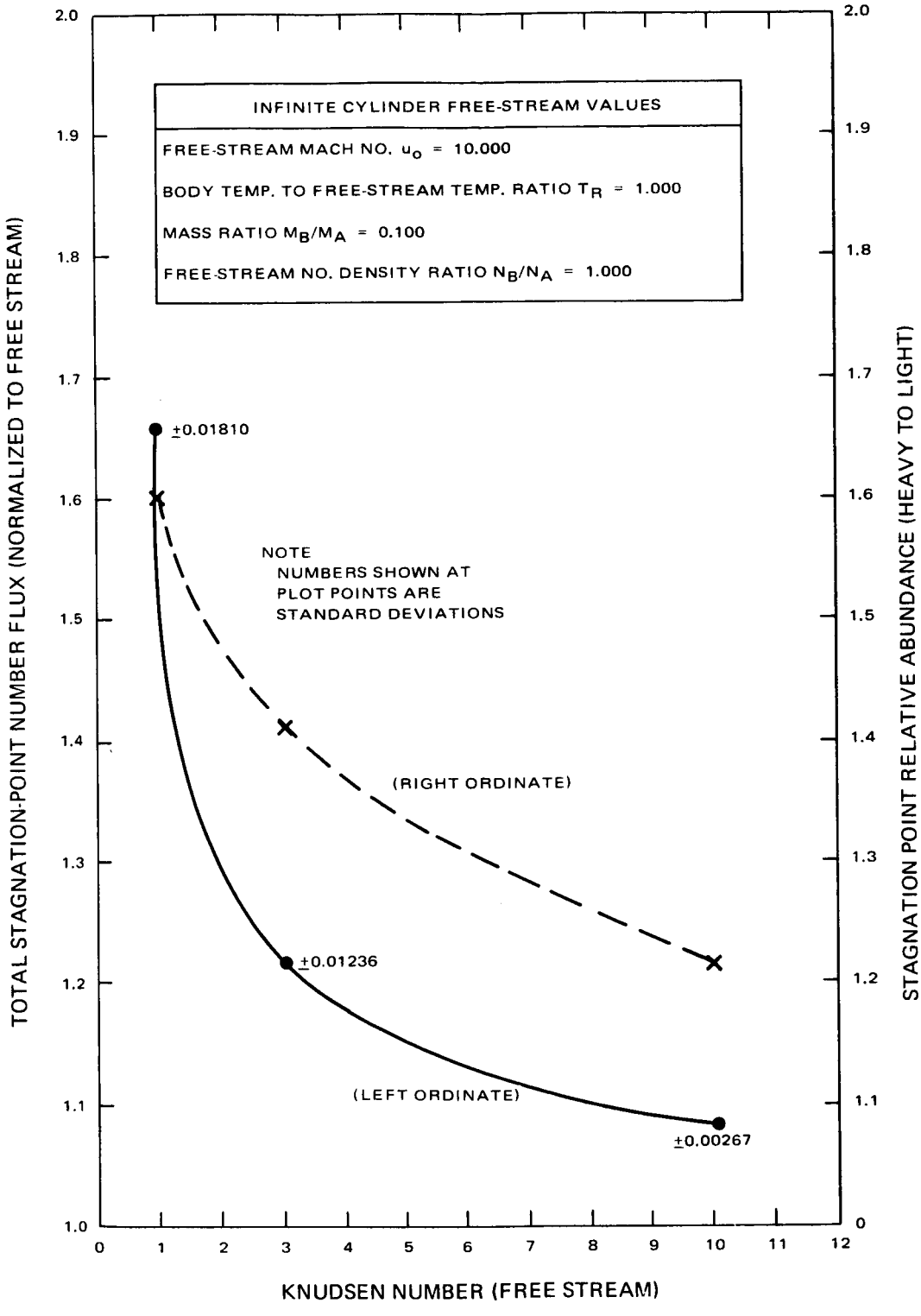


Figure 2. Behavior of Stagnation-Point Number Fluxes with Variation of the Free-Stream Knudsen Number ($N_B/N_A$ = 1.000)

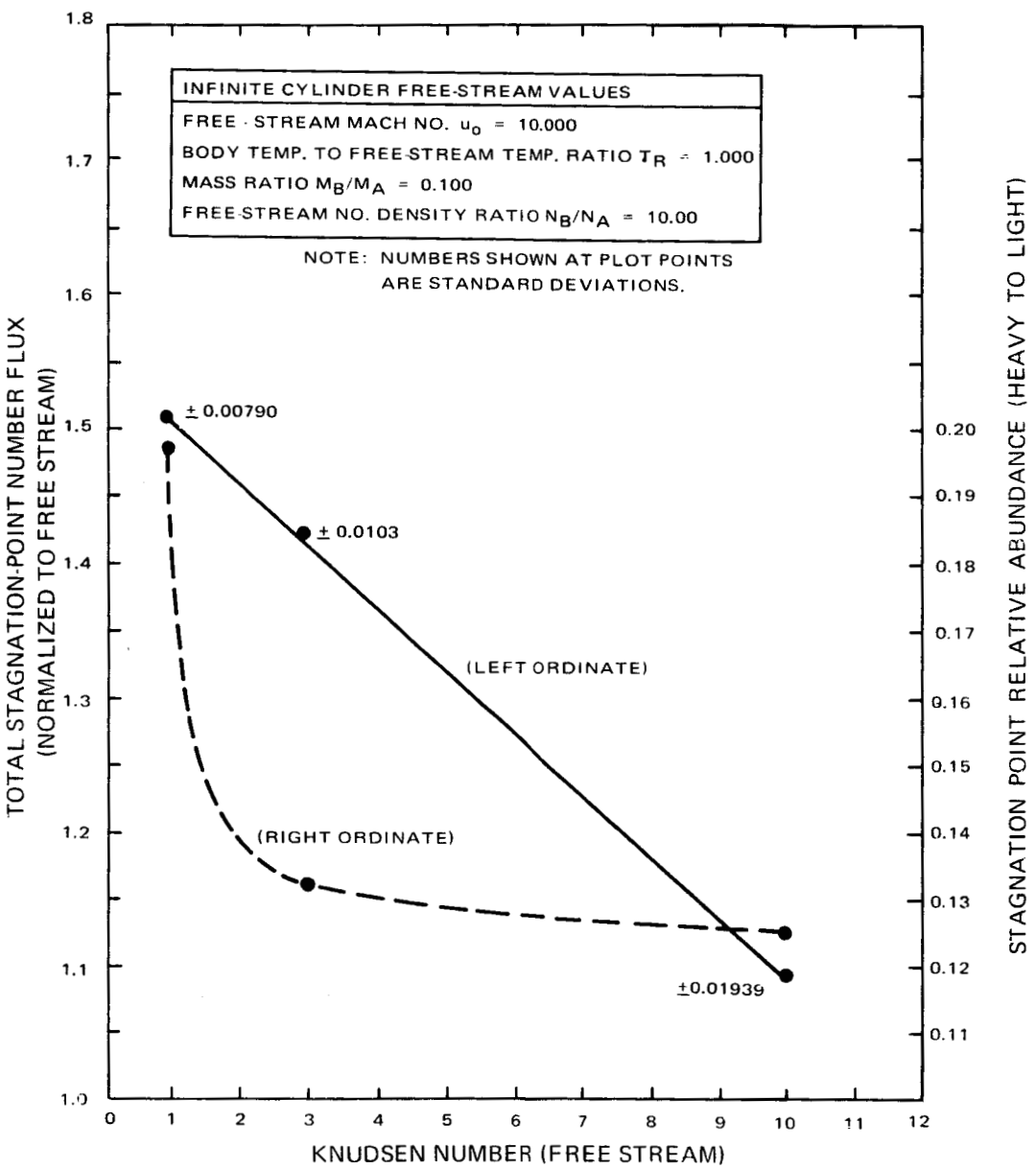


Figure 3. Behavior of Stagnation-Point Number Fluxes with Variation of the Free-Stream Knudsen Number ($N_B/N_A$ = 10.00)

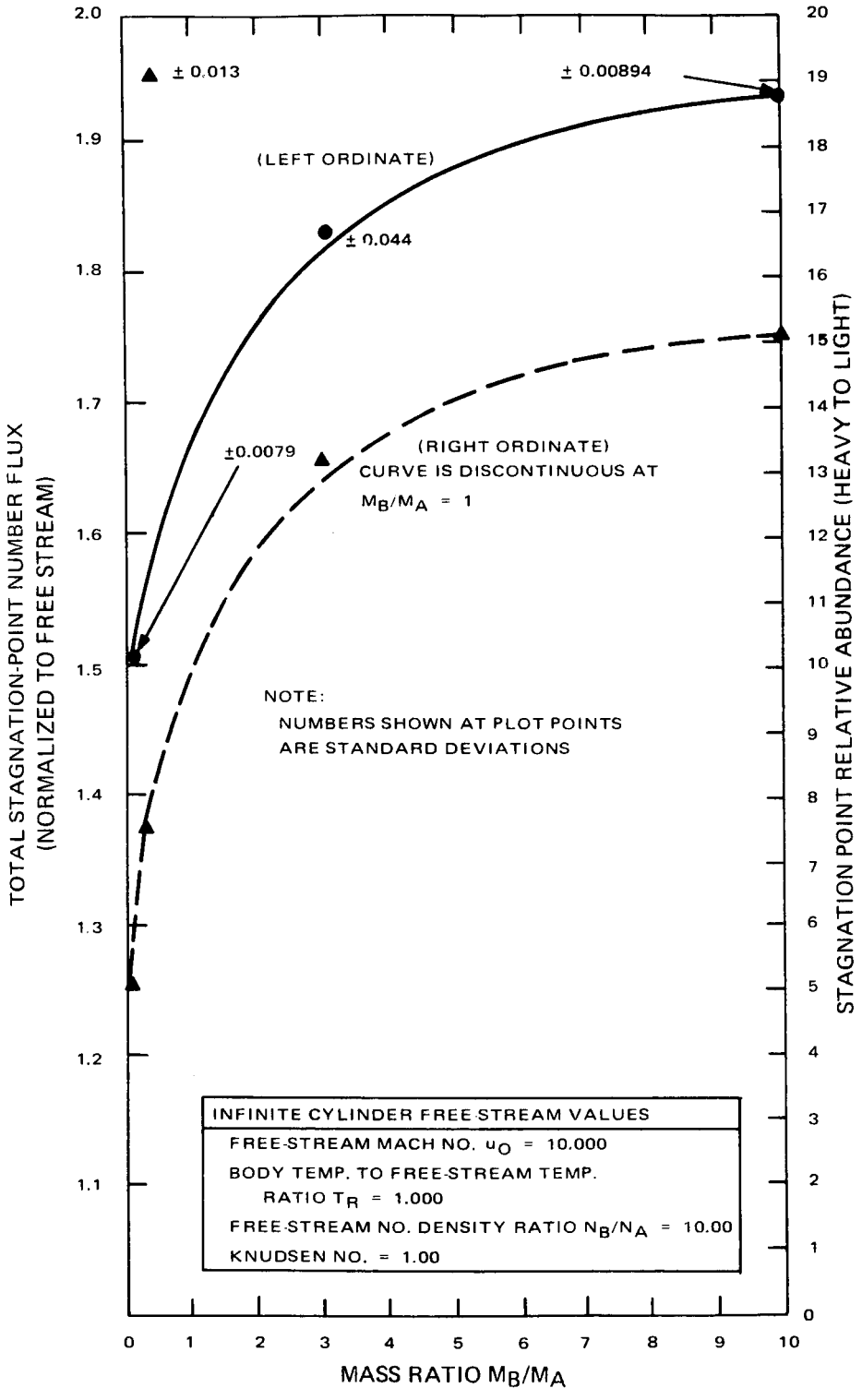


Figure 4. Behavior of Stagnation-Point Number Fluxes with Variation of Mass Ratio

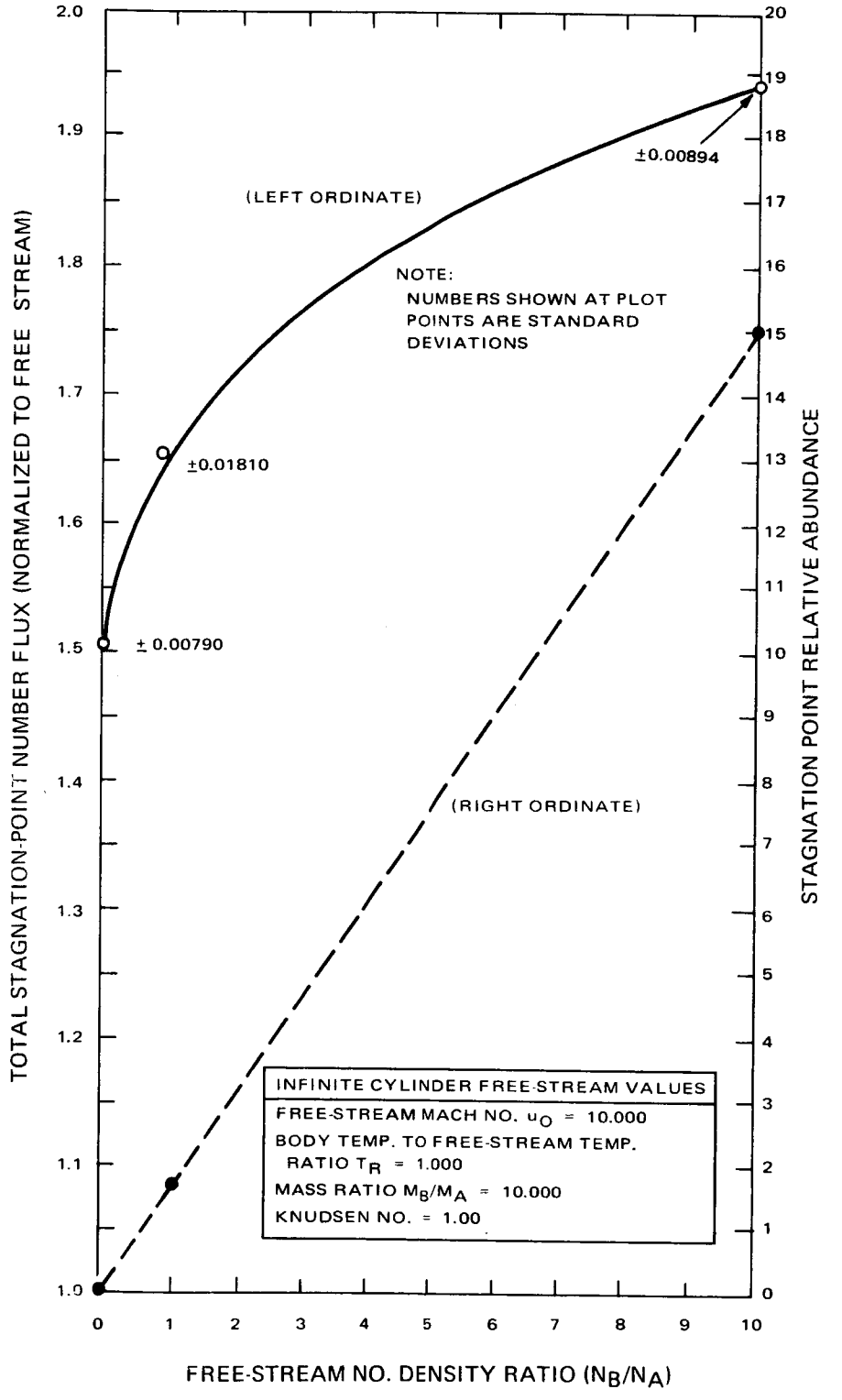


Figure 5. Behavior of Stagnation-Point Number Fluxes with Variation of the Free-Stream Number Density Ratio

TABLE 1. NUMBER FLUX DENSITY WITH VARIATION OF AZIMUTH ANGLE

Conditions:

Transverse cylinder flow

Free-stream Mach No. $u_o = 10.0$

Cylinder temp./gas temp. = 1.00

Free-stream no. density ratio $N_B/N_A = 1.00$

Mass ratio $M_B/M_A = 0.100$

Knudsen No. = 1.000

Standard deviation E is equal to 0.05316 for mixture number flux at $\theta = 0$.

| Azimuthal Angle $\theta$ (degrees) | Radial Number Flux* | | |
|---|---|---|---|
| | Mixture | Heavy Gas | Light Gas |
| 0.0 | 1.6561 | 1.0261 | 0.6300 |
| 10.0 | 1.6195 | 0.9565 | 0.6630 |
| 20.0 | 1.4991 | 0.8834 | 0.6157 |
| 30.0 | 1.3518 | 0.7513 | 0.6005 |
| 40.0 | 1.1734 | 0.6773 | 0.4961 |
| 50.0 | 0.9110 | 0.4801 | 0.4310 |
| 60.0 | 0.6951 | 0.3864 | 0.3087 |
| 70.0 | 0.4747 | 0.2409 | 0.2338 |
| 80.0 | 0.3025 | 0.1624 | 0.1401 |
| 90.0 | 0.1785 | 0.0866 | 0.0919 |
| 100.0 | 0.1071 | 0.0455 | 0.0616 |

*Normalized with respect to free-stream number flux.

TABLE 2. NUMBER FLUX DENSITY WITH VARIATION OF AZIMUTH ANGLE

Conditions:

Transverse cylinder flow

Free-stream Mach No. $u_o = 10.00$

Cylinder temp./gas temp. = 1.00

Free-stream no. density ratio $N_B/N_A = 10.00$

Mass ratio $M_B/M_A = 0.100$

Knudsen No. = 1.000

Standard deviation E is equal to 0.05252 for mixture number flux at $\theta = 0$.

| Azimuthal Angle $\theta$ (degrees) | Radial Number Flux* | | |
|---|---|---|---|
| | Mixture | Heavy Gas | Light Gas |
| 0.0 | 1.5078 | 0.2489 | 1.2589 |
| 10.0 | 1.5407 | 0.2234 | 1.3174 |
| 20.0 | 1.6056 | 0.2104 | 1.3952 |
| 30.0 | 1.2852 | 0.1772 | 1.1081 |
| 40.0 | 1.2127 | 0.1582 | 1.0545 |
| 50.0 | 0.9333 | 0.1124 | 0.8209 |
| 60.0 | 0.6721 | 0.0832 | 0.5889 |
| 70.0 | 0.4734 | 0.0467 | 0.4267 |
| 80.0 | 0.3363 | 0.0248 | 0.3115 |
| 90.0 | 0.1934 | 0.0084 | 0.1849 |
| 100.0 | 0.0899 | 0.0023 | 0.0876 |

*Normalized with respect to free-stream number flux.

TABLE 3. NUMBER FLUX DENSITY WITH VARIATION OF AZIMUTH ANGLE

Conditions:

Transverse cylinder flow

Free-stream Mach No. $u_o = 10.0$

Cylinder temp./gas temp. = 1.00

Free-stream no. density ratio $N_B/N_A = 10.00$

Mass ratio $M_B/M_A = 10.000$

Knudsen No. = 1.000

Standard deviation E is equal to 0.02875 for mixture number flux at $\theta = 0$.

| Azimuthal Angle $\theta$ (degrees) | Radial Number Flux* | | |
|---|---|---|---|
| | Mixture | Heavy Gas | Light Gas |
| 0.0 | 1.9368 | 1.8170 | 0.1197 |
| 10.0 | 1.7255 | 1.5964 | 0.1291 |
| 20.0 | 1.8000 | 1.6791 | 0.1209 |
| 30.0 | 1.4708 | 1.3644 | 0.1064 |
| 40.0 | 1.3185 | 1.2265 | 0.0920 |
| 50.0 | 1.0336 | 0.9604 | 0.0732 |
| 60.0 | 0.7915 | 0.7317 | 0.0599 |
| 70.0 | 0.4551 | 0.4105 | 0.0446 |
| 80.0 | 0.3201 | 0.2904 | 0.0297 |
| 90.0 | 0.1772 | 0.1590 | 0.0182 |
| 100.0 | 0.1084 | 0.0941 | 0.0143 |

*Normalized with respect to free-stream number flux.

TABLE 4. NUMBER FLUX DENSITY WITH VARIATION OF AZIMUTH ANGLE

Conditions:

Transverse cylinder flow

Free-stream Mach No. $u_o = 10.0$

Cylinder temp./gas temp. = 1.00

Free-stream no. density ratio $N_B/N_A = 10.00$

Mass ratio $M_B/M_A = 3.000$

Knudsen No. = 1.000

Standard deviation E is equal to 0.04015 for mixture number flux at $\theta = 0$.

| Azimuthal Angle $\theta$ (degrees) | Radial Number Flux* | | |
|---|---|---|---|
| | Mixture | Heavy Gas | Light Gas |
| 0.0 | 1.8323 | 1.7035 | 0.1288 |
| 10.0 | 1.7113 | 1.5704 | 0.1408 |
| 20.0 | 1.6537 | 1.5283 | 0.1254 |
| 30.0 | 1.5420 | 1.4244 | 0.1176 |
| 40.0 | 1.4113 | 1.3060 | 0.1053 |
| 50.0 | 1.1199 | 1.0286 | 0.0913 |
| 60.0 | 0.7685 | 0.7090 | 0.0595 |
| 70.0 | 0.5214 | 0.4737 | 0.0477 |
| 80.0 | 0.3198 | 0.2920 | 0.0277 |
| 90.0 | 0.1879 | 0.1703 | 0.0175 |
| 100.0 | 0.0995 | 0.0876 | 0.0118 |

*Normalized with respect to free-stream number flux.

TABLE 5. NUMBER FLUX DENSITY WITH VARIATION OF AZIMUTH ANGLE

Conditions:

Transverse cylinder flow

Free-stream Mach No. $u_o = 10.0$

Cylinder temp./gas temp. = 1.00

Free-stream no. density ratio $N_B/N_A = 10.00$

Mass ratio $M_B/M_A = 0.333$

Knudsen No. = 1.000

Standard deviation E is equal to 0.03544 for mixture number flux at $\theta = 0$.

| Azimuthal Angle $\theta$ (degrees) | Radial Number Flux* | | |
|---|---|---|---|
| | Mixture | Heavy Gas | Light Gas |
| 0.0 | 1.9530 | 0.2268 | 1.7262 |
| 10.0 | 1.7327 | 0.2125 | 1.5201 |
| 20.0 | 1.7234 | 0.2081 | 1.5153 |
| 30.0 | 1.4613 | 0.1585 | 1.3027 |
| 40.0 | 1.2455 | 0.1309 | 1.1146 |
| 50.0 | 0.9697 | 0.1082 | 0.8615 |
| 60.0 | 0.8319 | 0.0824 | 0.7495 |
| 70.0 | 0.4890 | 0.0477 | 0.4413 |
| 80.0 | 0.3373 | 0.0258 | 0.3115 |
| 90.0 | 0.1627 | 0.0102 | 0.1525 |
| 100.0 | 0.1274 | 0.0041 | 0.1233 |

*Normalized with respect to free-stream number flux.

TABLE 6. NUMBER FLUX DENSITY WITH VARIATION OF AZIMUTH ANGLE

Conditions:

Transverse cylinder flow

Free-steam Mach No. $u_o = 10.0$

Cylinder temp./gas temp. = 1.00

Free-stream no. density ratio $N_B/N_A = 1.00$

Mass ratio $M_B/M_A = 3.00$

Knudsen No. = 1.000

Standard deviation E is equal to 0.05357 for mixture number flux at $\theta = 0$.

| Azimuthal Angle $\theta$ (degrees) | Radial Number Flux* | | |
|---|---|---|---|
| | Mixture | Heavy Gas | Light Gas |
| 0.0 | 1.7721 | 1.0440 | 0.7281 |
| 10.0 | 1.6954 | 0.9191 | 0.7763 |
| 20.0 | 1.6615 | 0.9191 | 0.7424 |
| 30.0 | 1.4937 | 0.7977 | 0.6960 |
| 40.0 | 1.2626 | 0.6567 | 0.6059 |
| 50.0 | 1.0145 | 0.5497 | 0.4649 |
| 60.0 | 0.7424 | 0.4265 | 0.3159 |
| 70.0 | 0.5050 | 0.2534 | 0.2516 |
| 80.0 | 0.3649 | 0.1615 | 0.2034 |
| 90.0 | 0.1901 | 0.0955 | 0.0946 |
| 100.0 | 0.1133 | 0.0393 | 0.0741 |

*Normalized with respect to free-stream number flux.

Figures 2 and 3 present the variation in total number flux, and the ratio of the heavy to light specie flux at the stagnation point, with change of Knudsen number. The speed ratio is 10, the body temperature is the same as free-stream temperature and mass ratio is 0.1 in both cases. Figure 2 presents results for equal concentrations of both specie in the free stream; Figure 3 presents results for a 10-to-1 ratio of light to heavy free-stream gas abundance. The trends and orders of magnitude are approximately the same in both cases. The total flux increases with a decrease in Knudsen number. The relative abundance of the heavy gas is greater at the stagnation point than in the free stream; it also increases with decreasing Knudsen number. In the second case (Figure 3), where the light-gas concentration is larger, the overabundance of the heavy gas is more pronounced, especially at the lower Knudsen numbers.

Figures 4 and 5 summarize the variation of the stagnation point fluxes with mass ratio and concentration ratio in the free stream at a fixed Knudsen number of unity. Figure 4 presents the total flux and the ratio of the flux of specie B to that of specie A as a function of the mass ratio of specie B to specie A. (Note: As mass ratio goes through 1.0 from below, specie B changes from being the light to being the heavy gas.) At this Knudsen number of 1.0 and a 10-to-1 relative concentration in the free stream, the relative concentration at the stagnation point varies from about 5 to 15 as the mass ratio varies from 0.1 to 10. Figure 5 shows the variation of the fluxes at the stagnation point versus the ratio of fluxes in the free stream, at a Knudsen number of 1.0 and a mass ratio of 10. Note that the heavy specie is always overabundant compared to the free stream, the overabundance varying from about 95 percent when $N_B/N_A$ = 0.1 to about 50 percent when $N_B/N_A$ = 10. This would imply that, unless properly corrected, measurements on the vehicle would tend to overestimate the heavy-particle concentrations in the atmosphere.

In addition to the summaries of the fluxes at the stagnation point, the distribution of flux versus angle on the cylinder is given in Tables 1 through 6. Tables 7 through 9 give corresponding information for the sphere. Table 10 gives the value of stagnation point number flux density of the mixture for additional sets of values of the main parameters for the cylinder. Some care should be exercised in interpreting the data on angular distribution, as the accuracy depends upon computing time and azimuthal angle; it becomes quite low as the angle approaches 90 degrees. The trends in both absolute and relative abundances are expected to be correct. Figure 6 shows the variation of the total flux given in Table 1 normalized to the stagnation-point value. In addition, the variation in the free molecular ($K_n \simeq \infty$) and continuum ($K_n \simeq 0$) limits is shown. Although no absolute certainty of the validity of the present results can be obtained from this comparison, the fact that the angular distribution of the flux at a Knudsen number of 1.0, obtained in the present work, lies between the two limiting cases is very encouraging evidence of the basic validity of the program. Finally, Table 11 shows a very interesting two-gas effect. The flux is a maximum not at the stagnation point but at an angle in the vicinity of 20 degrees. As expected, the total pressure is a maximum at the stagnation point. The "ram" effect of the heavier

TABLE 7. NUMBER FLUX DENSITY WITH VARIATION OF AZIMUTH ANGLE

Conditions:

Sphere flow

Free-stream Mach No. $u_o = 10.0$

Sphere temp./gas temp. = 1.00

Free-stream no. density ratio $N_B/N_A = 10.00$

Mass ratio $M_B/M_A = 7.00$

Knudsen No. = 3.00

| Azimuthal Angle $\theta$ (degrees) | Radial Number Flux* | | |
|---|---|---|---|
| | Mixture | Heavy Gas | Light Gas |
| 0.0 | 1.1185 | 0.0934 | 1.0251 |
| 20.0 | 1.0961 | 0.0899 | 1.0062 |
| 40.0 | 0.8370 | 0.0663 | 0.7707 |
| 60.0 | 0.5645 | 0.0439 | 0.5206 |
| 80.0 | 0.2066 | 0.0188 | 0.1878 |
| 100.0 | 0.0241 | 0.0034 | 0.0207 |

*Normalized with respect to free-stream number flux.

TABLE 8. NUMBER FLUX DENSITY WITH VARIATION OF AZIMUTH ANGLE

Conditions:

Sphere flow

Free-stream Mach No. $u_o = 10.0$

Sphere temp./gas temp. = 1.00

Free-stream no. density ratio $N_B/N_A = 1.00$

Mass ratio $M_B/M_A = 7.00$

Knudsen No. = 3.00

| Azimuthal Angle $\theta$ (degrees) | Radial Number Flux* | | |
|---|---|---|---|
| | Mixture | Heavy Gas | Light Gas |
| 0.0 | 1.0309 | 0.5004 | 0.5304 |
| 20.0 | 0.9912 | 0.4485 | 0.5428 |
| 40.0 | 0.7976 | 0.3905 | 0.4071 |
| 60.0 | 0.5305 | 0.2462 | 0.2843 |
| 80.0 | 0.2001 | 0.0987 | 0.1014 |
| 100.0 | 0.0242 | 0.0156 | 0.0086 |

*Normalized with respect to free-stream number flux.

TABLE 9. NUMBER FLUX DENSITY WITH VARIATION OF AZIMUTH ANGLE

Conditions:

Sphere flow

Free-stream Mach No. $u_o = 5.00$

Sphere temp./gas temp. = 11.00

Free-stream no. density ratio $N_B/N_A = 1.00$

Mass ratio $M_B/M_A = 1.001$

Knudsen No. = 3.00

| Azimuthal Angle $\theta$ (degrees) | Radial Number Flux* | | |
|---|---|---|---|
| | Mixture | Heavy Gas | Light Gas |
| 0.0 | 1.0314 | 0.4584 | 0.5730 |
| 20.0 | 0.7473 | 0.4103 | 0.3370 |
| 40.0 | 0.6783 | 0.3158 | 0.3625 |
| 60.0 | 0.3819 | 0.2025 | 0.1794 |
| 80.0 | 0.1679 | 0.0916 | 0.0763 |
| 100.0 | 0.0153 | 0.0051 | 0.0102 |

*Normalized with respect to free-stream number flux.

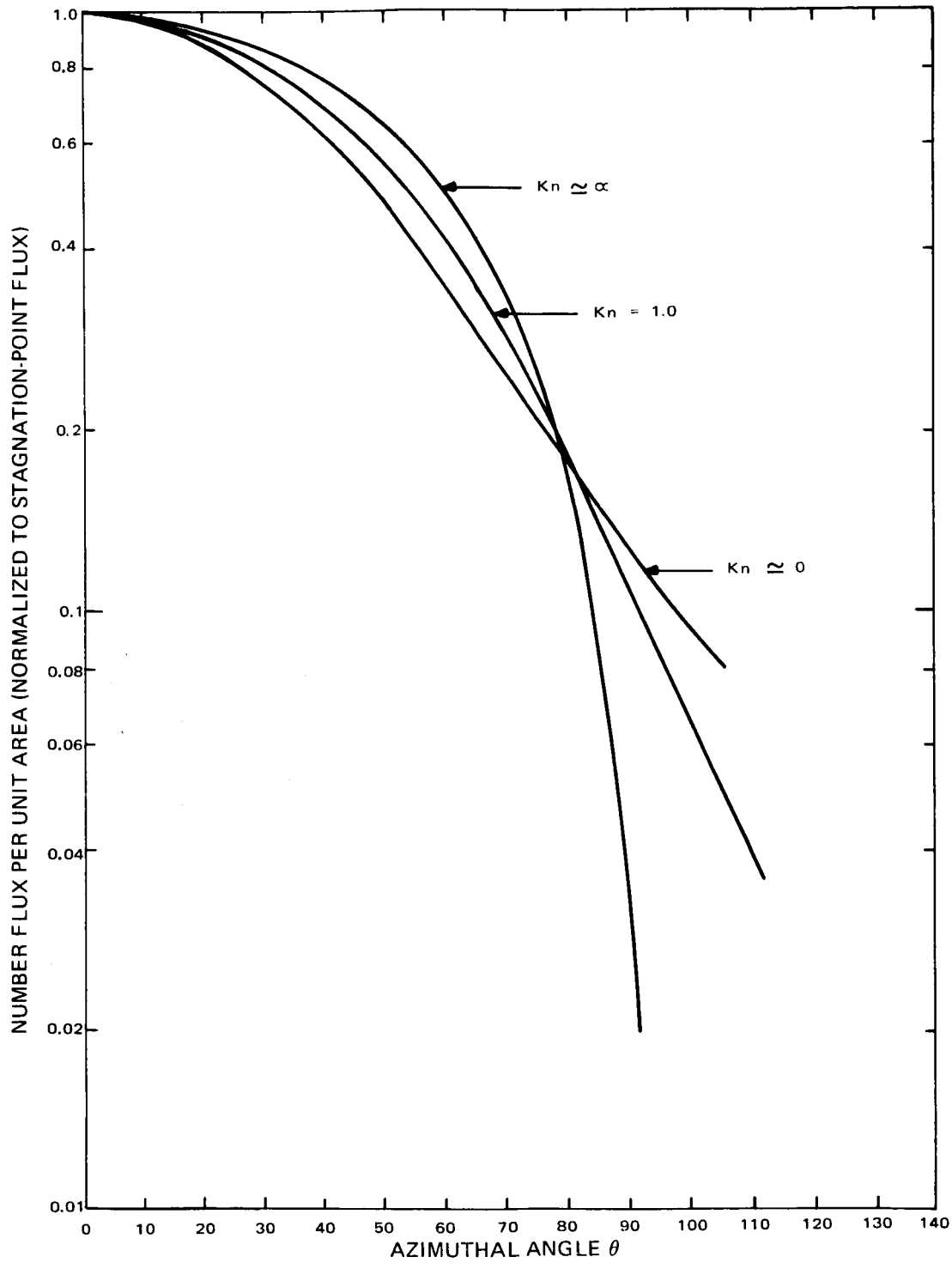


Figure 6. Stagnation-Point Number Flux Density as a Function of Azimuth Angle

TABLE 10. STAGNATION-POINT MIXTURE NUMBER FLUX FOR ADDITIONAL INTERESTING SETS OF PARAMETERS INVOLVING THE INFINITE CYLINDER

| Total Stagnation Point No. Flux | Knudsen No. | $M_B/M_A$ | $N_B/N_A$ | $T_R$ | $u_o$ |
|---|---|---|---|---|---|
| 0.7689 | 0.300 | 1.000 | 5.000 | 11.000 | 5.000 |
| 0.8718 | 0.300 | 0.100 | 1.000 | 11.000 | 5.000 |
| 1.7721 | 1.000 | 3.000 | 1.000 | 1.000 | 10.000 |
| 1.9530 | 1.000 | 0.333 | 10.000 | 1.000 | 10.000 |

TABLE 11. VARIATION OF LIGHT-GAS NUMBER FLUX WITH AZIMUTH ANGLE (Reference Table 2.)

| Light Gas Number Flux | Standard Deviation Based on Normal Distribution | Azimuth Angle (degrees) |
|---|---|---|
| 1.00 | ±0.007 | 0 |
| 1.11 | ±0.034 | 20 |
| 0.84 | ±0.039 | 40 |
| 0.47 | ±0.053 | 60 |
| 0.15 | ±0.094 | 90 |

molecules is apparently "pushing" the lighter molecules off to one side of the stagnation point. Larger angular excursions due to particle collisions between unlike particles is much more pronounced for the lighter particles than for the heavier particles.

## B. PERTURBATION PROCEDURE

The plots shown in Figures 7 through 9 are results calculated from the perturbation theory. The particular curves given show the inward radial number flux plotted as a function of Knudsen number. The values shown are normalized with respect to the free-stream flux.

The domain of validity of calculations based on the perturbation theory can be given in a semi-quantitative way by the expression $1 << r/a < L/a$, where a is typical vehicle dimension, L is the mean free path, and r is the distance from the body to the observation point. The expression simply indicates the region of space in the general vicinity of the vehicle for which valid calculations can be performed. (Thus, the ratio of the distance between the point of observation and the surface of the vehicle to a typical vehicle dimension must be considerably greater than 1.0. In addition, the local value of the mean free path and vehicle size must be such that their ratio, the Knudsen number, is in turn much greater than r/a.) Though the guide to the domain of validity is not very precise, a reasonable partial check as to when the condition is being violated can be had by examining the results of the calculations.

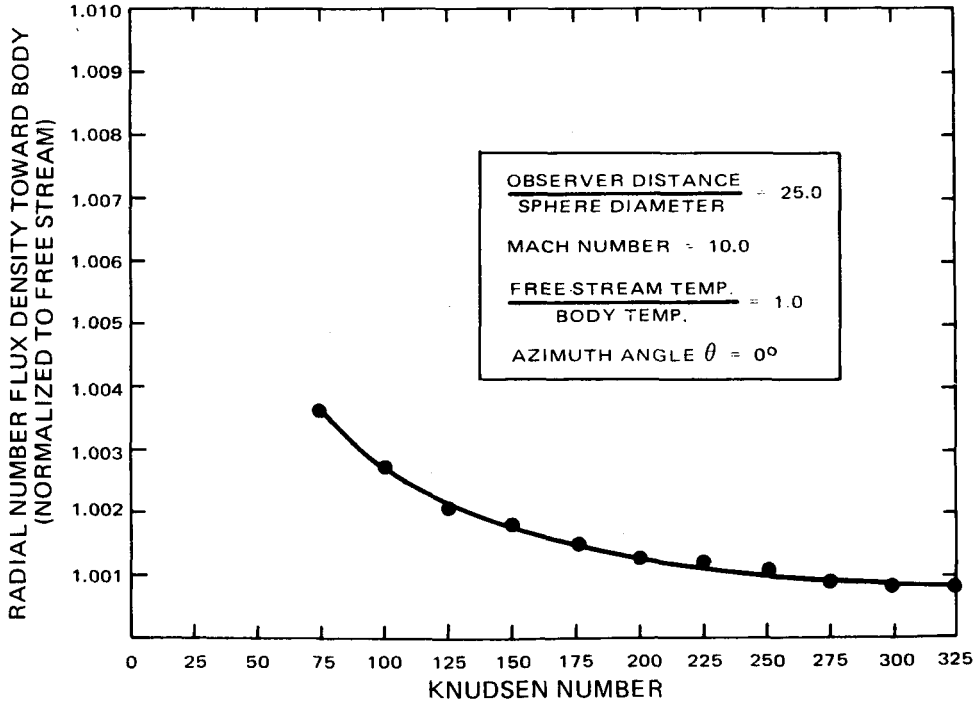


Figure 7. Radially Inward Number Flux for the Sphere (0° Azimuth Angle)

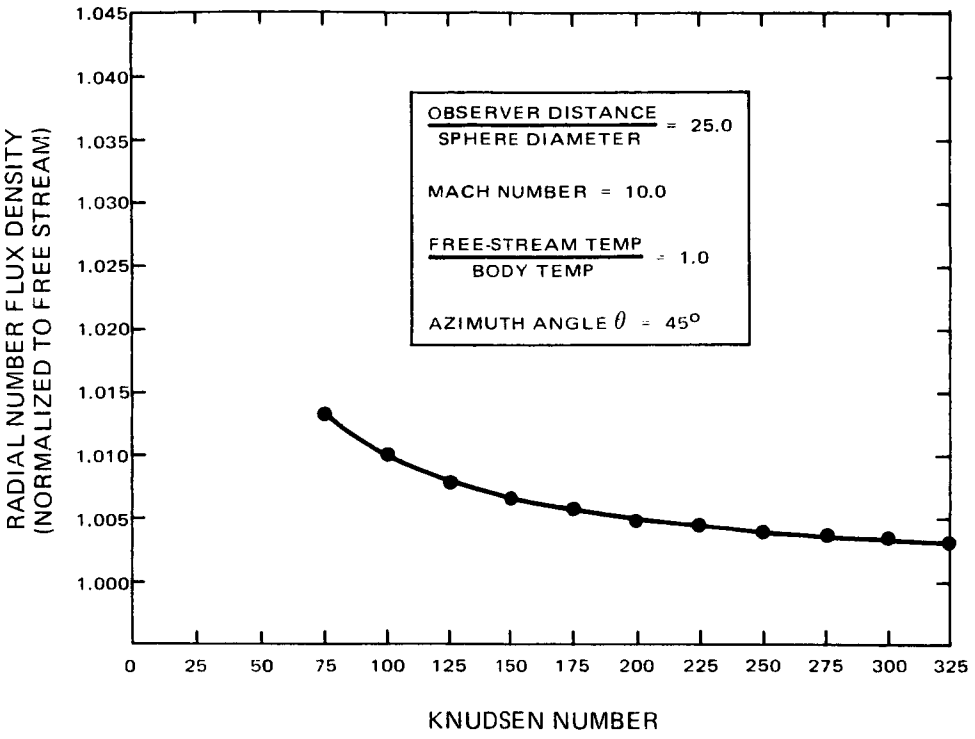


Figure 8. Radially Inward Number Flux for the Sphere (45° Azimuth Angle)

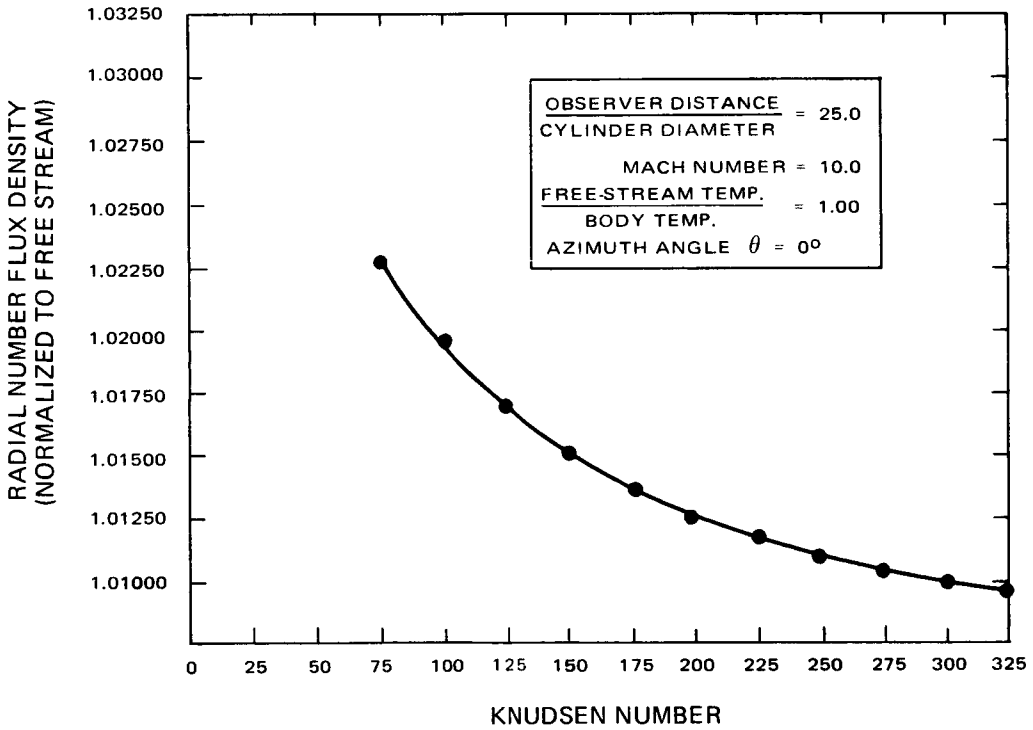


Figure 9. Radially Inward Number Flux for the Cylinder

Since the theory being discussed is a perturbation theory, the results of the calculations must give values that are reasonably small fractions of the free-stream values of the various quantities. This obviously does not provide a positive criterion of correctness; however, the contrary generally indicates incorrectness. A factor of 10 to 15 percent is usually regarded as a reasonable upper limit for calculated values using perturbation theory.

The curves in Figures 7 through 9 were evaluated for $(r/a) = 25.0$. The requirement for $(r/a) >> 1$ was imposed in order to avoid the geometric complexities inherent in the problem when distances away from the surface are on the order of a typical body length.

Although the actual values of the important parameters at the body surface such as number flux are not directly available from the perturbation calculation, they can be estimated on the basis of a simple model. If it is assumed that the molecules move without collisions from the points where the calculation is carried out to the body surface, the results of the perturbation calculation can be considered as indicative of the number flux at the body surface as well. On this basis, it is possible to compare the results of the Monte Carlo procedure with those of the perturbation technique.

It should be noted that the Monte Carlo calculations can give significant results only when the deviation from the free molecular value is greater than the standard deviation associated with the finite sample and time used for the calculation. The perturbation results, on the other hand, can only be considered valid when the perturbation from free molecular flow is small. Although a point by point comparison was therefore not possible, a comparison of the trends and the possibility of smooth transition from one to the other solution has been investigated.

Figure 10 shows the number density flux at a stagnation point on a cylinder normalized by the free molecular value, as a function of Knudsen number. The crosses indicate the Monte Carlo results, with the associated bars representing the standard deviation. For Knudsen numbers above 50, the perturbation results are presented in terms of a solid line with a cross-hatched area around it representing the estimated order of magnitude of the error arising from the higher order terms in the perturbation. Note that the basic trends given by both theoretical results are similar, and that at about a Knudsen number of 50 the two results lie within each other's error estimates. The dashed curve is drawn as a possible smooth curve which lies everywhere within the allowed error band. Although the comparison cannot be said to be conclusive, it does present additional evidence supporting the veracity of the Monte Carlo technique.

Another feature of the perturbation results derives from the way in which the radial number flux density decreases with increasing Knudsen number. As noted above, it is quite reasonable to assume that, as the Knudsen number varies, the comparative values of the number flux at the body surface and at the point evaluated would remain reasonably constant. If this is so, it suggests that the effects of transitional flow (i.e., of

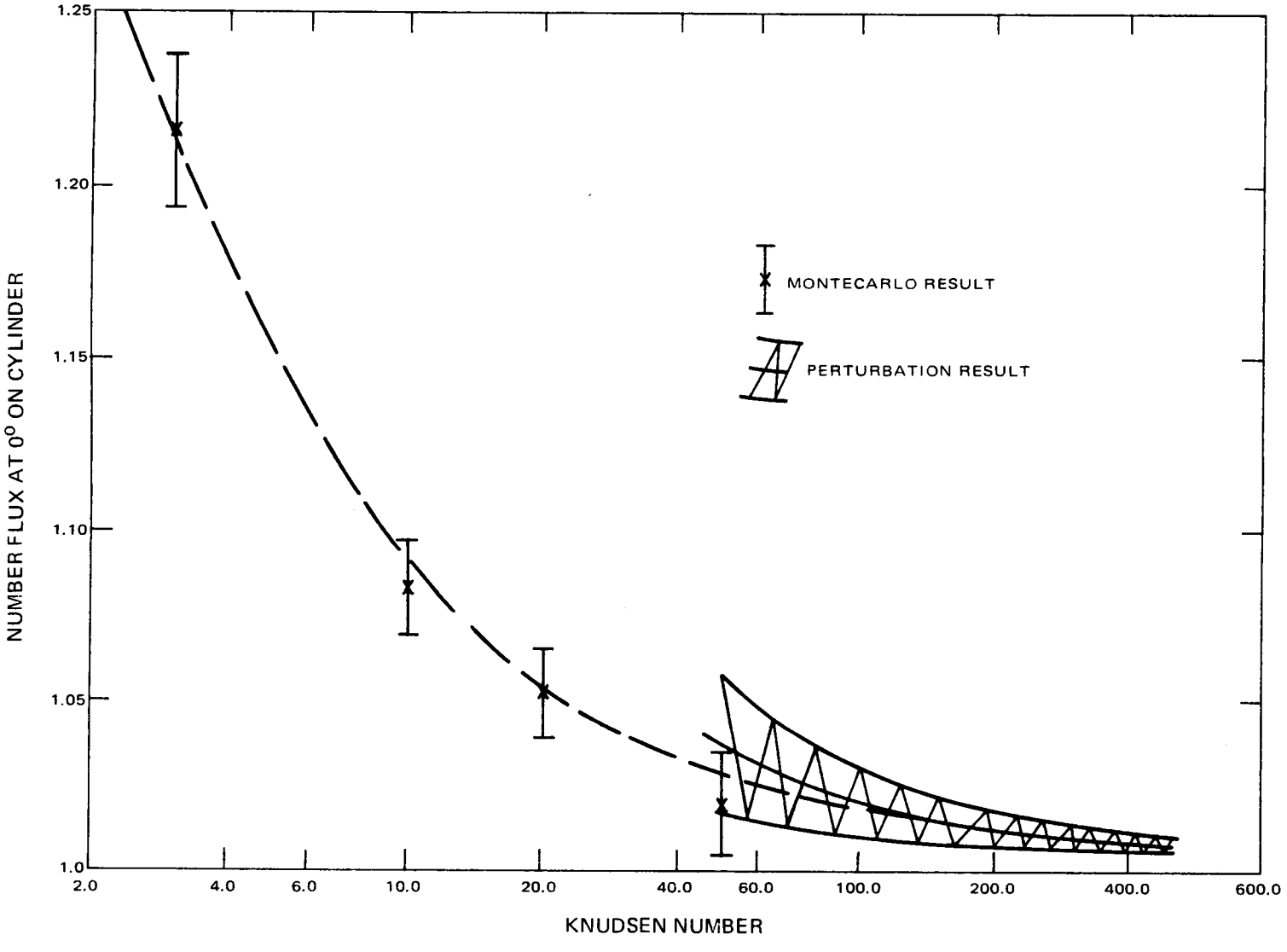


Figure 10. Comparison of Results from Both Monte Carlo Computations and Perturbation Theory

collisions) persist well beyond an altitude of 150 kilometers (supposing a mean free path of 25 meters and a 1-meter diameter sphere as the body). This level was previously thought to be a reasonable boundary altitude between transitional and free molecule flow for such a body. Such perturbation calculations for different shapes can orient the use of the Monte Carlo procedure as to the largest Knudsen number that must be calculated. Since increasing Knudsen number increases computer running time, and hence computer cost, at a fairly rapid rate, this guide can result in more efficient use of the computer program. At a later stage of programming development, checks can be built into the Monte Carlo computer program; these checks would obviate the need for using the perturbation theory. At present, however, perturbation calculations can help in the more efficient use of computer running time.

## C. AVAILABLE OUTPUTS FROM MONTE CARLO PROGRAMS

Because the sampling of the particles in the program is considered to correspond to the sampling of the distribution of particles in the model problem, any property obtainable from the distribution function is accessible as a possible output of the program. Of course, the more detailed the desired information, the more computer time must be used to obtain a specific accuracy. At present, all the printed outputs are confined to properties obtainable from integrals over the distribution function (moments). It is relatively easy to provide a more detailed structure of the distribution function itself as an output, but the time required to produce results with reasonable standard deviations increases proportionately to the resolution desired. For instance, if the distribution function of the flux of particles at the body surface was desired*, with a resolution of 10 divisions in the normal velocity, the computer time would be 10 times that required for the total flux computation. (With present accuracy requirements, this would imply about two hours of computing time for the cylinder.) Thus, although it may be desirable in a certain limited number of selected cases to obtain such detailed information, the production run outputs are confined to moments of the distribution function.

The moments selected for outputs in the present version of the program can be divided into three categories: overall integral quantities, surface flux distributions, and flow field moments. The first portion of the output consists of a presentation of the input parameters. Until steady flow is established, the outputs are only of diagnostic value. After steady flow is established, the information contains the averages over the sampled particles. For the largest available time these averages are considered to be the solution. An outline of the information contained in such an output is given below.

*This distribution would be needed for internal flow computations at the orifice of an instrument.

The output includes numbers denoting the instantaneous numbers of molecules in the whole working volume. It also includes the cumulative number of collisions between molecules and between molecules and the surface. These numbers are primarily of diagnostic value.

Another group of outputs consists of the overall integral quantities (such as the total flux, drag and heat transfer coefficients to the body). The normalizations are all in terms of the free-stream values. The number flux is normalized by the free-stream number flux per unit area times the projected body area. The drag is normalized by one-half the momentum flux in the conventional way, and the heat flux is normalized by the free-stream energy flux.

A set of data is provided to give the flux per unit area on segments of the surface. (For a cylinder, the segments are strips centered on the angular position, while for the sphere the segments are annular regions similarly centered.) Also given is the total number of molecules that have struck the surface up to that time. This value serves as a measure of the sample size on which the results are based. Additional data given for each unit area are the number flux, skin friction or tangential momentum flux, pressure or normal momentum flux, and heat transfer of energy flux. These values are normalized by the corresponding free-stream values. All the results are given for the mixture as a whole and for the light and heavy gas separately. This set of data is probably most relevant for the present purposes of the program, and the only information used in the summaries of the results.

Flow field information is included as an output. It provides conventional moments such as number density, mean velocities, and temperature, within each cell. All quantities are, as usual, normalized by their free-stream values. The information includes the cell number and the X and Y coordinates of the center of that particular cell. The origin of coordinates is at the center of the cylinder or sphere; X is always positive in the direction of the flow, and Y is perpendicular to it. The cumulative number of particles that have resided in the cell is also given. The averaging is based on this number and may be used to estimate the expected standard deviation of the results. Additional information provided is number density, X velocity, Y velocity, temperature, and the ratio of the number density of B molecules to that of A molecules. The mean thermal energy per particle, normalized by the free-stream value, is given for the X, Y, and Z directions, respectively. These results are included in order to provide a rough measure of the local non-equilibrium of the distribution functions, since at equilibrium all three values should be the same. The instantaneous population of each cell is also included for diagnostic purposes.

# SECTION VI
# CONCLUSIONS

The primary objective of the study was to provide a means of determining the relations between (1) state variables measured at an instrument on a rapidly moving vehicle, and (2) the corresponding values of the state variables in the free-stream (ambient atmosphere) and in the transition flow regime. This objective has been achieved.

The construction of a working "Monte Carlo" program for the sphere and cylinder has demonstrated the feasibility of the present approach and the accessibility of the transition region to detailed calculations. However, if the calculations are to have complete quantitative relevance to the data interpretation problem, the mode will require further sophistication. Operational experience with the present computational program indicates that, at least for geometries with some symmetry, sufficient sophistication can be added within available computer capabilities.

The limited information obtained on the results, both by the Monte Carlo technique and by the perturbation method indicate that the flow field can have a very great effect on data interpretation. As discussed in the results, there is a general tendency of the heavy specie to become overabundant in the stagnation point region. Data taken by an instrument placed there, if not properly interpreted, could lead to very erroneous conclusions about the relative concentrations within the atmosphere. Because the absolute values of the fluxes differ sufficiently from their free-stream values, improper interpretation of data could also lead to errors (up to factors of 2) in the number densities of the ambient atmosphere.

The present work has demonstrated operationally that the transition regime flow field studies are accessible by the "Monte Carlo" method. It has also shown the importance of such studies in the correct interpretation of data obtained from instruments of high-speed vehicles.

The prime criterion for instrument positioning derived from the calculations is the size of the standard deviation. Generally, an increase in the absolute number flux produces a corresponding increase in the statistical accuracy. This fact suggests that points close to the stagnation point (when there is only one) are optimum for instrument positioning. However, the statistical error in the correction factors given herein can be made small enough with sufficient computer time. Thus, the criterion suggests that the positioning of instruments, for the bodies considered, is not too critical from the standpoint of error.

From the point of view of composition measurement, an interesting situation has come to light. It has been determined that the position of greatest accuracy for the measurement of the relative abundance of two species depends upon their mass ratio. This is the so-called two-gas effect. Additional study will be required to determine optimum instrument position, but for certain mass ratios, it is probably not the stagnation point.

Error as a function of position is an important, but only partial, criterion for the choice of instrument position. In the final analysis, the selection of instrument position must involve detailed consultation between the instrument user, the instrument designer, and the vehicle designer. Nonetheless, the calculations contained herein provide very useful criteria for this selection and important corrections for the data reduction process.

# REFERENCES


1. Alder, B. J., and Wainwright, T. E., "Molecular Motions", Scientific American, October 1959.

2. D. H. Davis, Journal of Applied Physics, Vol. 31, p. 1169 (1960).

3. C. H. Kruger, M.I.T., Department of Mechanical Engineering Report No. DSR-7-8120, January 1960.

4. Troost, M., M.I.T. Thesis (1958).

5. Haviland, J. K., "Determination of Shock Wave Thicknesses by the Monte Carlo Method", Rarefied Gas Dynamics (ed. by J. A. Laurman), Academic Press, Inc., New York, 1963.

6. Bird, G. A., "Shock Wave Structure in a Rigid Sphere Gas", Rarefied Gas Dynamics (ed. by J. H. de Leeuw), Academic Press, New York, 1965, Vol. I, p. 216.

7. Bird, G. A., A.I.A.A. Journal, Vol. 4, p. 55 (1966).

8. Nordsieck, A., and Hicks, B. L., "Monte Carlo Evaluation of the Boltzmann Collision Integral", Rarefied Gas Dynamics, Academic Press, Inc., New York, 1967, Vol. I, p. 695.

9. Hammersley, J. M. and Handscomb, D. C., Monte Carlo Methods, Methuen and Co., Ltd., London, 1964.

10. H. Grad, "Equations of Flow in a Rarefied Atmosphere" NYO-2543 V, June, 1959. New York University, New York, N.Y.

11. M. Rose, "Drag on an Object in Nearly-Free Molecular Flow", Physics of Fluids, Vol. 7, p. 1262 (1964).

# APPENDIX I

# PERTURBATION PROCEDURE EMPLOYED IN DETERMINING FLUID FLOW QUANTITITES

## PART A

## MAJOR ANALYSIS

INTRODUCTION:

The purpose of this appendix is to acquaint the interested personnel with the details of a perturbation solution of the kinetic equation (Krook Model) involved in the problems of the study. As its purpose is largely didactic, a number of details concerning the background of the calculations will be dealt with at some length.

The particular calculation performed in this appendix is the evaluation to 2nd order in the peturbation, of the radial flux vector. A spherical body is assumed.

BACKGROUND OF THE PROBLEM:

Because of the range of values of the flow parameters inherent in this problem area, specialized techniques of solution are required. This problem falls into the so-called transitional flow region. This is a region in which the ratio of the mean free path in the free stream for collision between gas particles to a typical satellite dimension is of the order of unity. (This ratio is called the Knudsen number; designated Kn).

The transitional flow field contrasts with the free molecule flow field typical for satellites at higher altitudes for which the Knudsen number is very large (i.e, $Kn >> 1$). The essential mathematical difference is that the transitional flow field requires the retention of the collision term in the basic kinetic equation.

For transitional flow problems, the basic equation is the Boltzmann kinetic equation. For a multi-species gas*, the Boltzmann equation for the $i^{th}$ species is:

$$\frac{\partial f_i}{\partial t} + v_i \frac{\partial f_i}{\partial r_i} + \frac{F_i}{m_i} \frac{\partial f_i}{\partial v_i} = \sum_j \iiiint (f_i' f_j' - f_i f_j) \, k_{ij} \, dk \, dv_j \qquad (1)$$

where:

$f_i$ = distribution function of the $i^{th}$ species in velocity and configuration space (the superscript primes indicate post collision quantities).

$t$ = time

$v_i$ = instantaneous velocity of $i^{th}$ species

$r_i$ = position vector of $i^{th}$ species

$F_i$ = externally applied forces (throughout let $F_i = 0$)

$m_i$ = mass per particle of the $i^{th}$ species

$k_{ij}$ = the encounter variable for binary collisions between particles for the $i^{th}$ and $j^{th}$ species.

---

* "Though not required initially, a multi-species notation will be employed for use in later stages of this work."

The moments of interest are defined:

$$n_i = \int f_i \, dv_i = \text{number density of the } i^{th} \text{ species} \tag{2a}$$

$$\bar{v}_i = \frac{1}{n_i} \int f_i \, v_i \, dv_i = \text{mean velocity of } i^{th} \text{ species} \tag{2b}$$

$$u = \frac{1}{\rho} \sum_j n_j m_j \bar{v}_j = \text{mass averaged velocity in a multi species fluid containing } j \text{ distinct species} \tag{2c}$$

$$\rho = \sum_j n_j m_j = \text{total mass density in a multi-species fluid containing j distinct species} \tag{2d}$$

For a single species, $u = \overline{v_i}$

$$T_i = \frac{m_i}{3k n_i} \int (v_i - u)^2 f_i \, dv_i = \text{temperatures of } i^{th} \text{ species} \tag{2e}$$

$$T = \frac{1}{n} \sum_j n_j \frac{m_j}{2} \overline{(v_j - u)^2} = \text{temperature of fluid averaged over all species} \tag{2f}$$

$$n = \sum_j n_j = \text{total number density in a multi-species fluid containing j distinct species} \tag{2g}$$

$\overline{(v_i - u)}$ = diffusion velocity of $i^{th}$ species, i.e., relative to mass flow.

$dv_i = dv_{ix} \, dv_{iy} \, dv_{iz}$ (i.e., a volume element in velocity space).

$= v_{ir}^2 \, dv_{ir} \sin\theta \, d\theta \, d\phi$.

DETAILS OF SOLUTION OF EQUATION (1):

As it stands, (1) defies solution in most cases. This is primarily because of the term on the right hand side (i.e., the so-called collision term). A variety of procedures have been invented to circumvent the difficulties of handling the collision term. The procedured invoked here is to replace the collision term by the so-called Krook term. Though the use of the Krook term has been the subject of some theoretical criticism, it seems to work reasonably well in flow problems. In its simplest form (i.e., for a single species gas), the Krook term (really Bhatnager-Gross-Krook) is:

$$\nu_{ii} (f_{io} - f_i)$$

where:

$\nu_{ii}$ = average collision frequency of $i^{th}$ particle with another of the same species

$f_{io}$ = local Maxwellian distribution function of the $i^{th}$ species.

Thus, (1) becomes, (for $F_i = 0$), in the single species case:

$$\frac{\partial f_i}{\partial t} + v_i \frac{\partial f_i}{\partial r} = -\nu_{ii}(f_i - f_{io}) \tag{3}$$

The collision term in a multi-species gas mixture has a more complicated form but for purposes of exposition, details of the multi-species problem will be deferred.

Equation (3) (and its multi-species generalization) represents the basic equation to be employed for the perturbation solutions. The statement of the problem is not yet complete as the boundary conditions have yet to be specified. This is the satellite itself. Its surface represents a boundary; in fact "the" boundary. This boundary condition controls, locally, the value of the distribution function. To underscore its importance, it is the values of the moments in (2) evaluated in the vicinity of the body which are the critical parameters desired.

It is well known that a boundary condition can be represented as a source term or in engineering terminology, a forcing function. Equation (3) will then be rewritten to include the boundary condition in the form of a source term:

$$v_i \frac{\partial f_i}{\partial r_i} = \nu_{ii}(f_{io} - f_i) + H(v, r) \tag{4}$$

where $H(v, r)$ is the source term and the explicit time dependence has been dropped since the distribution is steady state.

Equation (4) will be solved under such conditions that an explicit expression for H will be given. To begin with, if on any arbitrarily small section of the boundary surface, the same velocity distribution emanates as from any other section, then H can be written as a product of a function of velocity and a function of position. (Variations on this condition could be exploited for experimental purposes). Secondly, the range of Knudsen number, as stated above, is given as the ratio of a free stream mean free path (L) to typical body dimensions (see Figure I-1). It will be bounded on the lower side by $Kn = L/a \approx 20$. This will permit of a distance D such that: $a \ll D \ll L$.

Defining a distance D (scale length of observation) will permit a bounding radius inside of which free molecular flow is substantially guaranteed. Free molecular flow occurs, strictly speaking, in the limit of infinite mean free path. Practically

speaking, free molecular flow can be said to occur in a region in which the effects of collisions are so small as to provide a negligible effect on the dynamics of a typical particle. That is to say, collisions occur, but so rarely that the collision term can be neglected in the governing equations.

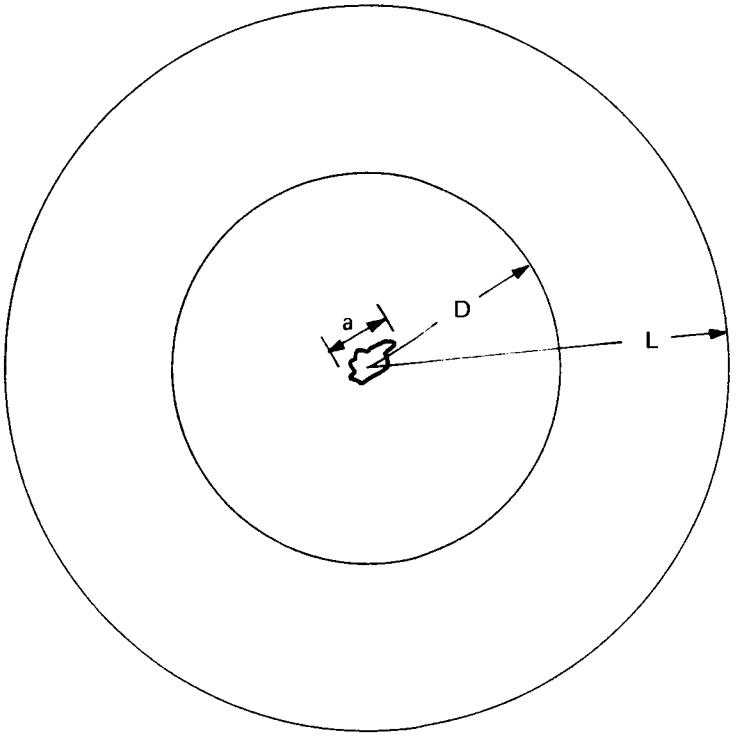


Figure I-1. Relationship of a, D, and L

In Figure I-1, a = characteristic body size,
D = the radius of the scale of observation,
L = the free stream mean free path.

Use will be made of the distance D later, but first development of (4) must proceed.

LINEARIZATION OF EQUATION (4):

Two basic modifications have yet to be made in Equation (4) before proceeding with solution: (1), the source term H(v, r) will be specified; (2) the equation itself will be linearized. As indicated above, under certain circumstances (and these will be invoked here), it is appropriate to write H(v, r) in the form of a product of two functions, one involving only velocities and one the configurational coordinates. Here, the boundary conditions to be imposed come into play in the way H(v, r) is to be written.

The actual physical condition at the boundary, of the interplay of impinging gas particle and the boundary surface, is a complicated dynamical problem in its own right. However, the detailed description of the dynamics and of the present level of understanding in this area, though important to the ultimate objective, is itself, not precisely relevent to present purposes. Phenomenological constants called "accommodation coefficients" will relate the properties of the input and output fluxes of the bounding surfaces. In particular, it will suffice for present purposes to assume a completely diffusive surface. For such a condition, regardless of the velocity distribution of the input flux, the effusive flux velocity distribution will be a 1/2 Maxwellian uniform over the body and following a simple cosine law (angle with respect to the local normal) for spatial flux distribution. (The above description is equivalent to setting the so-called accommodation coefficient equal to unity.)

On the above assumptions, one can write:

$$H(v, r) = \sigma(v)G(r).$$

G(r) = the bounding surface of the satellite. $\sigma(v)$ is the efflux velocity distribution function. On a scale of observation at a distance from the satellite of order a (see Figure I-1), all the geometric complexity of shape of the satellite is manifest. For $D >> a$, the details of the shape became less important in terms of the flux emanating from the surface and crossing say a surface of a unit volume a distance D from the satellite. In the limit, as D gets infinite, G effectively shrinks to a point.

This can be seen more clearly by considering the diagram shown in Figure I-2.

The component P' of the differential element of flux at a point P located at a distance D from the origin arising from an element of surface ds' located at M, is $dF_p$ where:

$$dF_p = M_f(\theta') \frac{ds'}{r^2} \cos \theta''$$

where $M_f(\theta')$ is the flux per unit area emanating from the surface located at an angle $\theta'$ and:

$$ds' = a^2 \sin \theta' \, d\theta' \, d\phi'$$

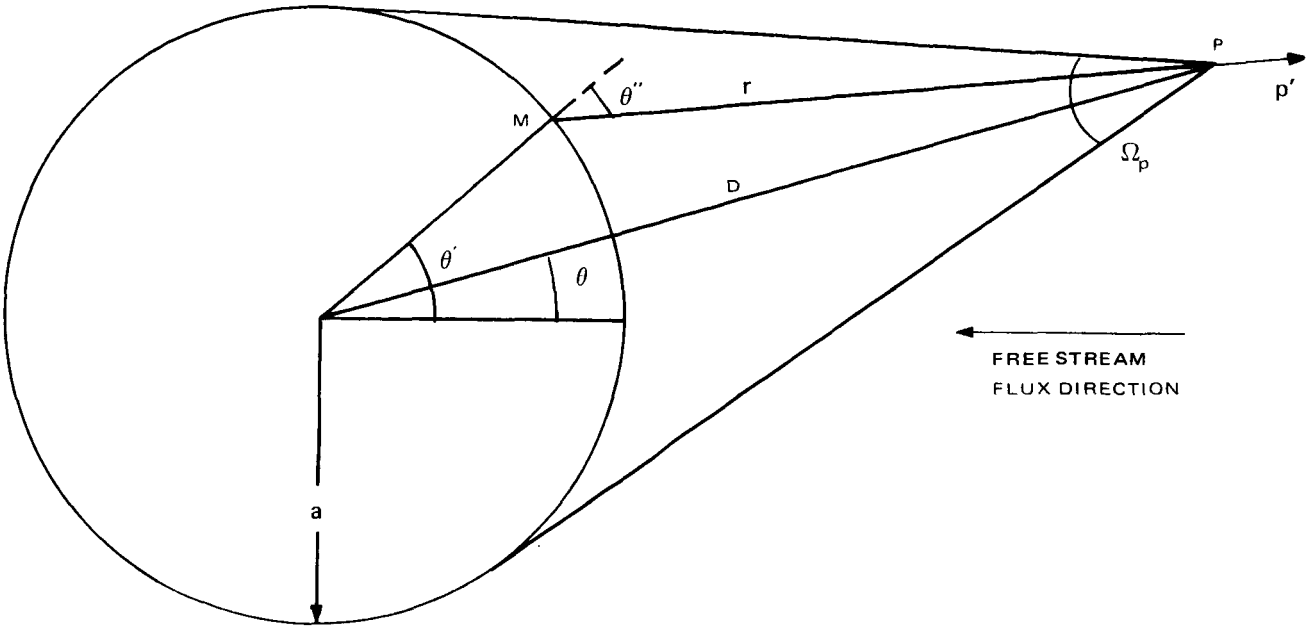


Figure I-2. Geometry Required to Describe the Flux to a Point P

and

$$r^2 = a^2 + D^2 - 2aD\cos(\theta' - \theta)$$

$$= D^2\left(1 + \frac{a^2}{D^2} - 2\frac{a}{D}\cos(\theta' - \theta)\right).$$

In the limit as the ratio a/D approaches zero,

$$r \to D \quad \theta' \to \theta \quad \theta' - \theta \to 0$$

$$dF_p \simeq M_f(\theta')\frac{a^2}{r^2}\sin\theta\, d\theta\, d\phi$$

and the cone defined by the solid angle $\Omega_p$ collapses into a ray.

The geometry required to describe the flux to a point P, reduces very considerably in complexity as P recedes to a distance D such that the ratio a/D gets very small. In effect, on a sphere of radius D in this approximation, the flux vector has only a radial component. On this basis, (i.e., as long as $a \ll D$) one can then approximate the physical extent of the body by a Dirac delta function. Hence, $G(\vec{r}) = \delta(\vec{r})$.

$$H(v, r) = \sigma(\nu_i)\delta_i(\vec{r}) \quad \lim a/D \to 0.$$

In the case that geometries other than a sphere are involved, the radius a is replaced by some characteristic length. Thus, for a cylinder, the cylinder diameter or length, whichever is the more appropriate, would replace the sphere diameter. This geometric approximation gives rise to the amended version of equation (4).

$$v_i \frac{\partial f_i}{\partial r} = \nu_{ii}(f_{io} - f_i) + \sigma_i(v_i)\delta(r_i) \tag{5}$$

It is the linearized form of (5) that is the basic working equation for the perturbation procedure. The linearization is straightforward. First, define the perturbation variables.

Let:

$$\begin{aligned}
f_i &= f_i^{(0)} + g_i = \text{distribution function} \\
n_i &= n_{io} + n_{il} = \text{number density} \\
m_i &= m_{io} + m_{il} = \text{mass of } i^{th} \text{ particle} \\
u_i &= u_{io} + u_{il} = \text{average velocity} \\
T_i &= T_{io} + T_{il} = \text{temperature} \\
P_i &= P_{io} + P_{il} = \text{pressure}
\end{aligned}$$

The subscripts io indicate free stream values of $i^{th}$ species. The i1 subscripts denote the perturbed values of $i^{th}$ species. (6)

The local Maxwellian $f_{io}$ is defined as:

$$f_{io} = \frac{n_i}{(2\pi \frac{k}{m_i} T_i)^{3/2}} \exp\left\{-\frac{(v_i - u_i)^2}{2(\frac{k}{m_i})T_i}\right\} \tag{7}$$

k is the Boltzmann constant.

Equation (7) can be linearized in terms of the free stream maxwellian $f_i^{(0)}$

where:

$$f_i^{(0)} = \frac{n_{io}}{(2\pi \frac{k}{m_i} T_{io})^{3/2}} \exp\left\{-\frac{(v_i - u_{io})^2}{2\frac{k}{m_i}T_{io}}\right\} \tag{8}$$

that is:

$$f_{io} = f_i^{(0)} \left\{ 1 + \frac{n_{il}}{n_{io}} + \left( \frac{c_i^2}{2R_iT_{io}} - \frac{3}{2} \right) \frac{T_{il}}{T_{io}} + \frac{(c_i \cdot u_{i1})}{R_iT_{io}} \right\} \tag{9}$$

where: $c_i = v_i - u_{io}$

and: $R_i = k/m_i$

In equations (5) thru (8), a number of quantities have been introduced. It is actually more convenient to deal with non-dimensional quantities.

Note the following definitions of dimensionless quantities:

$$\tilde{n}_i = \frac{n_i}{n_{io}}, \tilde{\rho}_i = \frac{\rho_i}{\rho_{io}}, \tilde{u}_i = \frac{u_i}{\sqrt{R_iT_{io}}}, \tilde{T}_i = \frac{T_i}{T_{io}}, \tilde{u}_{io} = \frac{u_{io}}{\sqrt{R_iT_{io}}}$$

$$\tilde{u}_i = \frac{u_i}{\sqrt{R_iT_{io}}}, \tilde{c}_i = \tilde{v}_i - \tilde{u}_{io}, \tilde{g}_i = \frac{(R_iT_{io})^{3/2}}{n_{io}} g_i$$

$$\omega_i = \frac{1}{(2\pi)^{3/2}} \exp \left\{ -\frac{\tilde{c}_i^2}{2} \right\} = \frac{(R_iT_{io})^{3/2}}{n_{io}} f_i^{(0)}$$

$$\tilde{\sigma}_i = \frac{(R_iT_{io})^{3/2}}{n_{io}} \sigma_i, \nu_{ii}/(R_iT_{io})^{1/2} = 1/L_{ii} \tag{10}$$

Employing equations (5) thru (10), the basic working equation (single species form) is arrived at.

$$\tilde{v}_i \frac{\partial \tilde{g}_i}{\partial r_i} + \frac{\tilde{g}_i}{L_{ii}} = \frac{\omega_i}{L_{ii}} \left\{ \tilde{n}_{i1} + \left( \frac{\tilde{c}_i^2}{2} - \frac{3}{2} \right) \tilde{T}_{il} + \tilde{c}_i \cdot \tilde{u}_{il} \right\} + \sigma_i \delta(r_i) \tag{11}$$

In terms of the dimensionless perturbed distribution function, $\tilde{g}$, the various appropriate dimensionless moments become:*

---

* The Analysis up to and including (12) is due to H. GRAD "Equations of Flow in a Rarefied Atmosphere": NYO-2543.

$$\tilde{n}_{il} = \int \tilde{g}_i d\tilde{v}_i = \text{(perturbed nondimensional number density)}$$

$$\tilde{u}_{ilk} + \tilde{n}_{il}\,\tilde{u}_{iok} = \int \tilde{v}_{ik}\tilde{g}_i d\tilde{v}_i \quad \text{(perturbed nondimensional number flux in k-direction)} \tag{12}$$

$$\tilde{T}_{il} = \int \left(\frac{\tilde{c}_i^2}{3} - 1\right) \tilde{g}_i d\tilde{v}_i = \text{(perturbed nondimensional temperature of } i^{\underline{th}} \text{ species)}$$

Following the usual procedure of integrating along the streamlines, examination of (11) suggests that the integration is to be carried out along the direction of the vector $\tilde{v}_i$. The value of $g_i$ at some arbitrary point P must come from integration along the direction of the fixed vector $\tilde{v}_i$. Thus, consider the following coordinate transformation:

$$\vec{r}_i = \vec{r}_{io} - \vec{\tilde{v}}_i s \quad \text{where } -\infty \leq s \leq \infty .$$

Here, $\vec{r}_{io}$ is a fixed vector from the origin to the point of observation P and $\vec{\tilde{v}}_i s$ is the vector from the variable source point to the point of observation. Here $\vec{\tilde{v}}_i$ is an arbitrary but fixed vector and s is a variable scalar magnitude. Now,

$$\frac{\partial \tilde{g}_i}{\partial r_i} = \frac{\partial \tilde{g}_i}{\partial s}\,\frac{\partial s}{\partial r}$$

and

$$s = \frac{(\vec{r}_{io} - \vec{r}_i) \cdot \vec{\tilde{v}}_i}{(\tilde{v}_i)^2}$$

so

$$\left(\frac{\partial s}{\partial \vec{r}}\right) = -\frac{\vec{\tilde{v}}_i}{(\tilde{v}_i)^2}$$

or

$$\tilde{v}_i \cdot \frac{\partial \tilde{g}_i}{\partial r_i} = -\frac{d\tilde{g}_i}{ds}$$

So that (11) becomes:

$$-\frac{d\,\tilde{g}_i}{ds} + \frac{\tilde{g}_i}{L_{ii}} = \frac{\omega_i \tilde{G}_i}{L_{ii}} + \tilde{\sigma}_i \frac{\delta(y_1 - y_1')\,\delta(y_2 - y_2')\,\delta(y_3 - y_3')}{h_1 h_2 h_3} \tag{13}$$

where the delta function has been volume normalized to unity by the metrical coefficients ($h_1\ h_2\ h_3$). Multiplying (13) thru by the integrating factor $e^{-S/L}$, and integrating over ds, it becomes:

$$\int_{S_o}^{\infty} \frac{d}{ds}\left(\tilde{g}_i\left(e^{-S/L_i}\right)\right) ds = \int_{S_o}^{\infty} \left(\frac{\omega_i}{L_{ii}}\,\tilde{G}_i + \tilde{\sigma}_i\,\frac{\delta(y_1-y_1')\,\delta(y_2-y_2')\,\delta(y_3-y_3')}{h_1h_2h_3}\right) e^{-S/L}\,ds \qquad (14)$$

A generalized lower limit has been assigned to the integrals corresponding to the specific conditions (e.g., boundary conditions) to be examined.

Integrating the left hand side of (14), one obtains:

$$\tilde{g}_i = + e^{So/L_{ii}} \int_{So}^{\infty} \left(\frac{\omega_i}{L_{ii}}\,\tilde{G}_i + \tilde{\sigma}_i\,\frac{\delta(x-x_1')\,\delta(x_2-x_2')\,\delta(x_3-x_3')}{h_1h_2h_3}\right) e^{-S/L_{ii}}\,ds \qquad (14a)$$

The integrand in (14a) suggest an iteration procedure in which equal orders in $(1/L_{ii})$ are equated

Now assume

$$\tilde{g}_i = \tilde{g}_{io} + \frac{1}{L_{ii}}\,\tilde{g}_{i1} + \text{H.O.T}$$

$$\tilde{G}_i = G_{io} + \frac{1}{L_{ii}}\,\tilde{G}_{i1} + \text{H.O.T.}$$

$$\tilde{\sigma}_i = \tilde{\sigma}_{io} + \frac{1}{L_{ii}}\,\tilde{\sigma}_{ii} + \text{H.O.T.}$$

( Where order (n+1) of $\tilde{\sigma}$ and order (n-1) of $\tilde{G}_i$ are obtained from order (n) of $\tilde{g}_i$. )

Expanding the exponents in the integrand in (14a), one obtains in lowest order of $(1/L_{ii})$:

$$\tilde{g}_{io} = \int_{S_o}^{\infty} \tilde{\sigma}_{io}\,\frac{\delta(x_1-x_1')\,\delta(x_2-x_2')\,\delta(x_3-x_3')}{h_1h_2h_3}\,ds \qquad (15)$$

where, as will be seen below, $\tilde{\sigma}_{io}$ is known, as it is determinable from the free stream flow. It is the lowest order approximation to the number flux off the sphere per unit velocity interval. $\tilde{g}_{io}$ is the lowest order approximation to the perturbation of the distribution function and is the free molecular flow perturbation. The coordinate transformation used to express (11) in the form (13) shows in general that the integration over the three independent space coordinates can be reduced to integration over one independent coordinate (i.e. the characteristic direction). Furthermore, invoking the geometrical approximation inherent in Fig. I-2, it becomes possible for $r >> a$ to approximate the stream lines, at least in the limit of free molecular flow, as purely radial lines. Thus even though the "sources" of g may be a function of $\theta$ (physically this refers to the fact that the efflux from the sphere is function of $\theta$), the integration can be done along a radial line.

For this situation (15) becomes

$$\tilde{g}_{io} = \int_o^{r'} \tilde{\sigma}_{io} \frac{\delta(r - r')\,\delta(\theta - \theta')}{\tilde{v}_{ir} 2\pi r'^2 \sin\theta'}\, dr' \tag{16a}$$

Integrating the sources of $\tilde{g}_{io}$ over the source coordinates and for $r' > r$

$$\tilde{g}_{io} = \frac{\tilde{\sigma}_{io}\,\delta(\theta - \theta')}{\tilde{v}_{ir} 2\pi r^2 \sin\theta'} \tag{16b}$$

BOUNDARY CONDITIONS:

Consider next the evaluation of $\tilde{\sigma}_{io}$. This is the net number flow in the free molecule flow approximation. In the case of a sphere, the free molecule component of the perturbed net flow can be seen graphically in Fig. I-3. The perturbed mass flow in the free molecule approximation at a point P, is the flow off the sphere (called B) minus the component of free stream flow (called C) which is prevented from arriving at P due to the presence of the sphere. The flow (called A) is not involved but is just the mean free stream flow direction. The flow (called C) which is a component of the free stream flux to P is subtracted out due to the presence of the sphere. It arises from those free stream particles with velocities directed toward P with magnitudes greater than the mean flow velocity. This is due to the thermal distribution of velocities. However, except for angles very close 180° in the hypersonic limit it is reasonable to ignore the flow called C.

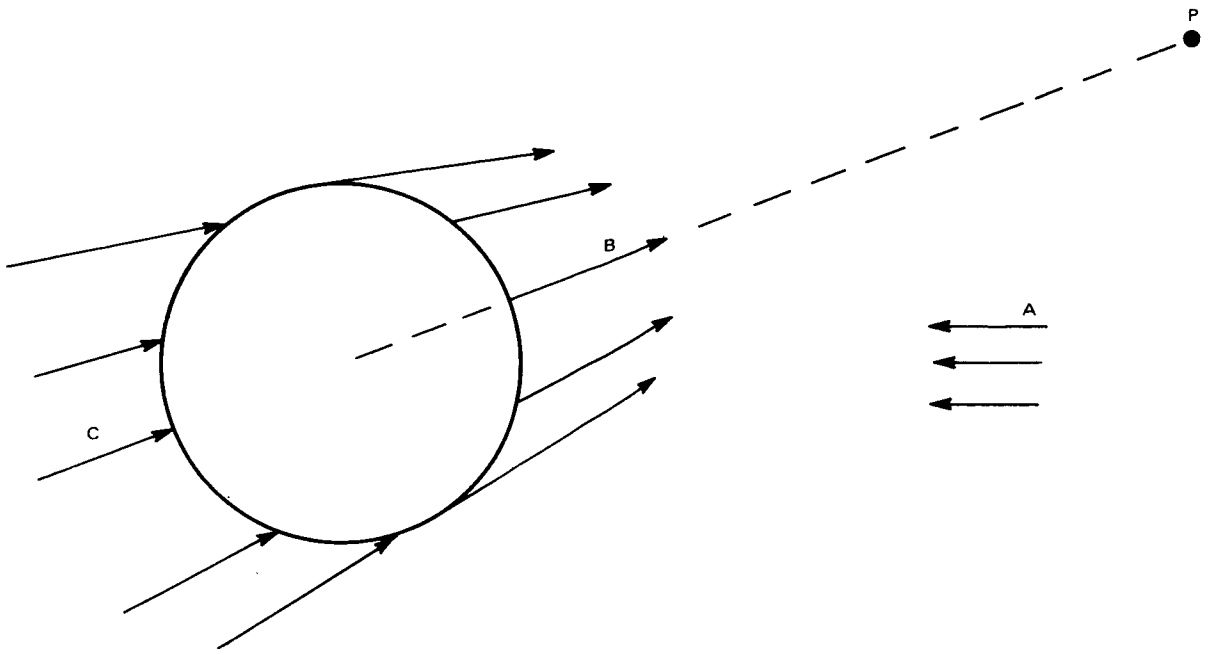


Figure I-3. Geometry for Computing the Effective Free-Molecular Source Strength $\tilde{\sigma}_{io}$

The function $\tilde{\sigma}_i$ for which the function $\tilde{\sigma}_{io}$ is the free molecular perturbation approximation, is defined as:

$$\tilde{\sigma}_i = \int \left(\tilde{g}_i\right)_B \tilde{v}_{ir}\, dS \qquad \text{(where dS is an element of the boundary surface).} \tag{17}$$

The quantity $(g_i)_B$ is the velocity distribution of the flux emanating from the boundary. Now:

$$(g_i)_B = \frac{n_f}{(2\pi R_i T_B)^{3/2}} e^{-v_i^2/2 R_i T_B} \tag{18}$$

where $n_f$ is an effective "areal" density such that $n_f v_{ir}$ is the number flux per unit area with a normal velocity $v_{ir}$ emanating from the body. $T_B$ is the body temperature. In the lowest order of perturbation, the effective flux from the body is:

$$\sigma_{io} = \int_o^{\pi} \frac{n_{f^{(o)}} v_{ir}}{(2\pi R_i T_B)^{3/2}} e^{-v_i^2/2 R_i T_B} 2\pi a^2 \sin\theta \, d\theta \qquad (19)$$

where $n_{f^{(o)}}$ is the lowest order approximation to $n_f$.

The general definition of $\sigma_i$ requires integration over the entire surface of the sphere because, as stated above, the perturbation has both a positive and negative contribution. But, in the hypersonic limit, only for angles very close to 180° is it necessary to include the "negative" contribution to the perturbation.

It is also clear that the so called "positive" area of interest on the sphere is that area which is visible at the observation point P, as other parts of the sphere cannot contribute particles to the perturbation at P in the free-molecule approximation. (In this limit, collisions in space do not contribute to the perturbation.) Additionally, not all areas of the sphere visible at P can supply particles because the particles originally derive from the free stream and the free-stream flux only contributes particles to that hemisphere of the surface facing the free stream. Thus, the actual area of integration becomes that area which is simultaneously seen from both the free stream direction and the observation direction. In the diagram of Figure I-4, this area is outlined with a dotted line.

As can be seen in Part C of this appendix the hypersonic limit approximation ($\tilde{u}_o >> 1$) fails at or very near 90°. In addition at or very near 180° the calculation is also invalid, as at 180°, even in the hypersonic limit, the flow (called C) cannot be ignored. These shortcomings in the calculations can be remedied but only at considerable additional effort and so will be ignored for present purposes.

In the hypersonic limit (see Part C) the term $\tilde{n}_{f(o)}$ is given as

$$\tilde{n}_{f(o)} = \frac{n_{f(o)}}{n_{io}} = \left(\frac{\pi}{2}\right)^{1/2} (\tau)^{1/2} \tilde{u}_o \cos\theta \qquad (20a)$$

The dependence on $(\tau)^{1/2}$ ($\tau = T_{io}/T_B$), the ratio of temperature of the free stream and the body, and on cos $\theta$ is expected on a simple physical basis. The presence of cos $\theta$ in equation (20) accounts for its presence in the integral formulation Part B of this appendix for the projection in a direction $\theta$ of the simultaneously visible area.

$\tilde{\sigma}_{io}$, the normalized total flow off the portion of the surface seen at P per unit velocity interval is (see Part B)

$$\tilde{\sigma}_{io} = \frac{(\tau)^2}{8\pi} \tilde{u}_{io}\, \pi a^2\, (1+\cos\theta)\, \tilde{v}_{ir}\, e^{-\tau/2\, \tilde{v}_i^2} \tag{20b}$$

(NOTE: $\tilde{\sigma}_{io}$ has the units of area; the normalized delta function used above has the units of a reciprocal volume.) The zero order perturbation function $\tilde{g}_{io}$ can now be written explicitly for the case of a sphere:

$$\tilde{g}_{io} = \frac{\tilde{u}_{io}\, \pi a^2 (1+\cos\theta)\, (\tau)^2\, \tilde{v}_{ir}\, e^{-\tau/2\, \tilde{v}_i^2}}{8\pi\ 2\pi\ \tilde{v}_{ir}\ r^2 \sin\theta}\, \delta(\theta - \theta') \tag{21}$$

Using the zero order i.e. $\tilde{g}_{io}$ and Equation (12), the zero order perturbation number density $n_{ilo}$ can be written:

$$n_{ilo} = \int \tilde{g}_{io}\, d\tilde{v}_i \qquad \text{which can be written} \tag{22}$$

$$n_{ilo} = \frac{u_{io}\, \pi^{1/2}\, (\tau)^{1/2}\, a^2 (1+\cos\theta)}{8\ (2)^{1/2}\ r^2} \tag{23}$$

The first moment of the number flux in the radial direction is

$$\tilde{u}_{ilor} = \int \tilde{v}_{ir}\, \tilde{g}_{io}\, d\tilde{v}_i - n_{ilo}\, \tilde{u}_{ior} \tag{24}$$

(where: $\tilde{u}_{ilor} = -\tilde{u}_{io} \cos\theta$)

$$\tilde{u}_{i10}\ r = \frac{a^2(1+\cos\theta)\, \tilde{u}_{io}}{8\, r^2} \left[ 2 + \frac{\tilde{u}_{io} \cos\theta}{2^{1/2}}\, (\pi)^{1/2}\ (\tau)^{1/2} \right] \tag{25}$$

$$\tilde{T}_{ilo} = \int \left( \frac{\tilde{c}_i^2}{3} - 1 \right) \tilde{g}_{io} \, d\tilde{v}_i \tag{26}$$

$$T_{ilo} = \frac{\tilde{u}_{io}(\tau)^{1/2} a^2 (1+\cos\theta)}{16 r^2} \left(\frac{2}{3}\right) \left[ \frac{3}{\sqrt{2}} \left(\frac{\pi}{\tau^2}\right)^{1/2} - \frac{4\tilde{u}_o \cos\theta}{(\tau)^{1/2}} + \frac{1}{\sqrt{2}} (\tilde{u}_{io}^2 - 3)\pi^{1/2} \right] \tag{27}$$

All the terms in the first term on the right hand side of Equation (11) have been determined to zero order in the perturbation.

$$\frac{\omega i}{L_{ii}} \tilde{G}_{io} = \frac{\omega i}{L_{ii}} \left\{ \tilde{n}_{ilo} + \left( \frac{\tilde{c}_i^2}{2} - \frac{3}{2} \right) \tilde{T}_{ilo} + \tilde{c}_i \cdot \tilde{u}_{ilo} \right\} \tag{28}$$

where the $\tilde{G}_{io}$ is the zero order perturbation value of $\tilde{G}_i$. Having evaluated $\tilde{G}_{io}$, the quantity $\tilde{g}_{ii}$ can be evaluated. In accordance with ordering the solutions in $1/L_{ii}$, $\tilde{g}_{i1}$ becomes

$$\begin{aligned} \tilde{g}_{il} &= \int_{(r')} \omega_i G_{io}(r) \frac{dr}{v_{ir}} \\ &+ \int_{(r')} \tilde{\sigma}_{io} \frac{\delta(r-r')\delta(\theta-\theta')(r'-r)dr'}{v_{ir} r'^2 \sin\theta} \end{aligned} \tag{29}$$

where only the first integral contributes to $\tilde{g}_{i1}$. In general, $\tilde{g}_{in} = \tilde{g}_{in}(\tilde{G}_{i(n-1)}, \tilde{\sigma}_{in})$. Eq. (29) becomes

$$\tilde{g}_{il} = \int_0^{r'} \omega_i \tilde{G}_{io}(r') \frac{dr'}{\tilde{v}_{ir}} \tag{30}$$

Integration of Equation (30) will proceed as in the case of (11) in a radial direction but for somewhat different reasons. The term in the integral in Equation (30) is a part of the collision term (i.e., producing particles for the distribution f). At distances $r >> a$, and greater, only a radial component of s is required as stream lines oriented, even at small angles with respect to a radial line, will result in the production of particles which miss the body by a significant distance. On the other hand at distances r small compared to D (i.e., $r \cong a$), all lines from a point P that land on the sphere are

valid directions of integration. In this latter regime, however, collisions are assumed to be negligible. Explicit recognition of this is observed as it is contained in the expansion variable; that is, the term $e^{-S/L}$ is expanded. It must be remembered that $\tilde{g}_{il}$ must be multiplied by (a/L) before it becomes the second approximation to $\tilde{g}_i$. By integrating along a radial line to a point r, an estimate to order a/L of the effects due to collisions contributing to $\tilde{g}_{il}$ is obtained. It must be recognized that to order (a/L), a relatively poor approximation is had to the true perturbation variables for any r which is not much greater than a.

Thus:
$$\tilde{g}_{il}(r, \theta, \tilde{v}_{ir}) = \frac{\omega_i \pi r^3}{v_{ir}} \tilde{G}_{io}(r, \theta, v_{ir}) \tag{31}$$

The radial component of the first perturbation away from the free stream value of the radial component of the flux $\tilde{u}_{il\,r}$ at the surface of the sphere is

$$\tilde{u}_{il\,r} = \int \tilde{v}_{ir}\, \tilde{g}_{il}\, d\tilde{v} - \tilde{n}_{il}\, \tilde{u}_{io\,r} \tag{32}$$

The calculations required in order to convert from a spherical to a cylindrical geometry are presented in Part C of this appendix.

# APPENDIX I

## PART B

## CALCULATION OF EFFECTIVE SOURCE AREA

In connection with Figure I-4, let A be the portion of the surface area of the sphere which is simultaneously visible to the free stream direction ($\theta = 0$), and to a point P at an arbitrary angle $\theta$ and at a distance from the origin r such that $r >> a$. As a result of $r >> a$, the difference between the portion of the surface area of the sphere which can be seen at P and the surface area of a hemisphere is negligible and it will be ignored. Let C be the surface area of the hemisphere which is visible to the free stream direction and B be the portion of the hemisphere C which can not be seen at P. Thus,

$$C - B = A, \text{ and}$$

$$C_P - B_P = A_P$$

where $A_P$ is the quantity to be evaluated. The subscripted values, i.e. $A_P$, $B_P$, $C_P$, denote the projections of A, B, and C, respectively, in the direction $\theta = 0$. Evidently, $C_P = \pi a^2$.

Let $\vec{n}$ be the unit vector in the direction of $\overrightarrow{OP}$.

$$n_x = \sin\theta \cos\phi$$

$$n_y = \sin\theta \sin\phi$$

$$n_z = \cos\theta$$

In order to obtain $B_p$ and hence $A_p$, it is necessary to obtain the expression for a great circle of the sphere whose plane is perpendicular to the unit vector $\vec{n}$.

Let Q be an arbitrary point on the great circle with coordinates:

$$Q_x = a \sin\theta' \cos\phi'$$

$$Q_y = a \sin\theta' \sin\phi'$$

$$Q_z = a \cos\theta'$$

Since the vectors $\vec{n}$ and $\vec{Q}$ are orthogonal, we have $\vec{n} \cdot \vec{Q} = 0$ or

$$\cos\phi \cos\phi' + \sin\phi \sin\phi' + \text{ctn}\,\theta \,\text{ctn}\,\theta' = 0 \qquad (33)$$

For computing the area $B_P$, the angle $\phi$ is immaterial and can be set equal to $\pi/2$, hence:

$$\text{ctn}\,\theta' = -\tan\theta \sin\phi' \text{ or}$$

$$\theta' = \text{ctn}^{-1}\,(k \sin\phi') \tag{34}$$

where $k = -\tan\theta$. Equation (34) is the expression for the great circle desired.

With the expression for the great circle known, the area $B_P$ can be expressed by the integral:

$$B_P = a^2 \int_0^{\pi} \int_{\theta_0(\phi')}^{\pi/2} \cos\theta' \sin\theta' \, d\theta' \, d\phi' \tag{35}$$

where $\theta_0$ is given by Eq. (34), i.e., $\theta_0 = \text{ctn}^{-1}\,(k \sin\phi')$. After carrying out the $\theta'$ - integration, Eq. (35) becomes:

$$B_P = \frac{a^2}{2} \int_0^{\pi} \left[1 - \sin^2\theta_0(\phi')\right] d\phi'$$

$$= \frac{a^2}{2} \left[\pi - \int_0^{\pi} \sin^2 \text{ctn}^{-1}\,(k \sin\phi')\, d\phi'\right] \tag{36}$$

Since:

$$\text{ctn}^{-1}\,(k \sin\phi') = \sin^{-1} \frac{1}{\sqrt{1 + k^2 \sin^2\phi'}}$$

it follows:

$$B_P = \frac{a^2}{2} \left[\pi - \int_0^{\pi} \frac{d\phi'}{1 + k^2 \sin^2\phi'}\right] \tag{37}$$

The integral in Eq. (37) can be evaluated immediately by the thereom of residues in the complex plane:*

Now Equation (37) also can be written as:

$$B_P = \frac{\pi a^2}{2} \cdot \left[1 - \frac{1}{\sqrt{1 + k^2}}\right]$$

The desired projection $A_P$ is:

$$A_P = C_P - B_P = \pi a^2 - \frac{\pi a^2}{2}\left[1 - \frac{1}{\sqrt{1 + k^2}}\right]$$

$$= \frac{\pi a^2}{2}\left[1 + \frac{1}{\sqrt{1 + k^2}}\right]$$

$$= \frac{\pi a^2}{2}\left[1 + \text{Cos } \theta\right] \qquad (38)$$

since $k = -\tan \theta$.

---

* The integral in Equation (37) also can be written as

$$\int_0^{\pi} \frac{d\phi'}{1 + k^2 \sin^2 \phi'} = 2\int_0^{\pi/2} \frac{d\phi'}{1 + k^2 \sin^2 \phi'}$$

The last integral can be found in Nouvelles Tables d' Integrals Defines, by D. de Haan.

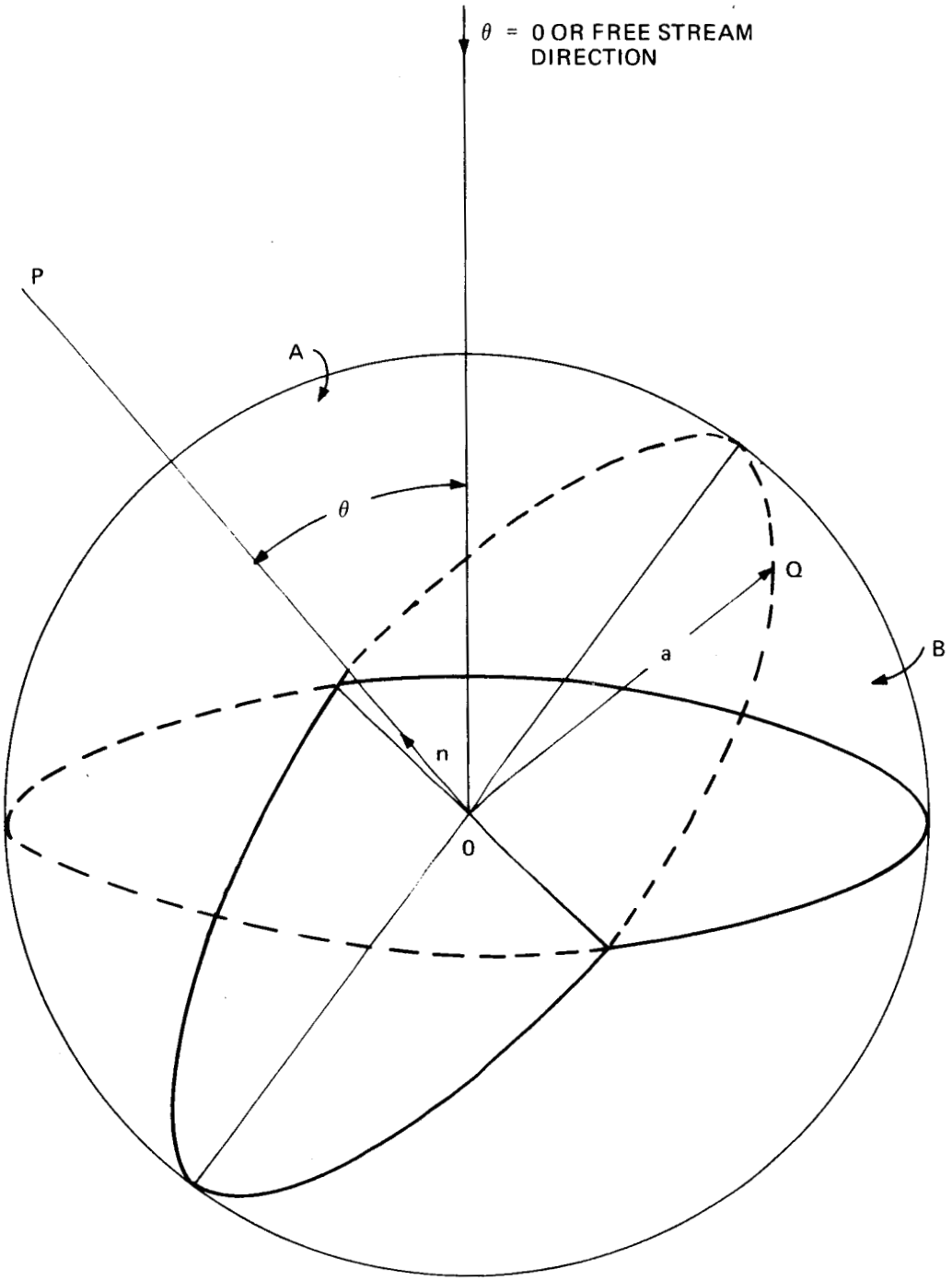


Dotted line parallels the line defining that portion of the surface of the sphere whose projection is of interest.

Figure I-4. Geometry for Calculation of Effective Source Area

# APPENDIX I

## PART C

## CALCULATION OF EMITTED FLUX DENSITY

In order to evaluate $\delta_{io}$, the quantity $n_e$ must first be obtained. In order to obtain the expression for

$$n_e \equiv n_f^{(0)} \text{ (Part A of this Appendix)}$$

which is the number of molecules per unit volume residing on the surface of the body, $n_e$ is most appropriately expressed in terms of $n_i$ where $n_i$ is the number of the molecules per unit volume in the in coming flux arriving at the body. The following consideration is given. Let the number of molecules per unit volume whose components of velocity lie in the range $v_1$, $v_2$, $v_3$ to $v_1 + dv_1$, $v_2 + dv_2$, $v_3 + dv_3$ be given by

$$dn = n\, f(v_1, v_2, v_3)\, dv_1\, dv_2\, dv_3 *$$

Let Ie be the flux of molecules (number of molecules per unit time per unit area) emitted from the sphere. Employing spherical coordinates in the velocity space, we have

$$I_e = \int v_r\, dn_e = \int_0^\infty \int_0^{2\pi} \int_0^{\pi/2} n_e v_r\, f(v)\, v_r^2 \sin\theta\, d\theta\, d\phi\, dv_r \tag{39}$$

where

$$f(v) = \exp\left(-v_r^2/2RT_B\right)/(2\pi RT_B)^{3/2} \tag{40}$$

After carrying out the $\theta$- and $\phi$- integrations, Eq. (39) becomes

$$I_e = \frac{2\pi n_e}{(2\pi RT_B)^{3/2}} \int_0^\infty v_r^3 \exp\left(-v_r^2/2RT_B\right) dv_r \tag{41}$$

* For simplification of notation the species subscripts are dropped in this calculation.

Let $T_B$ be the temperature of the body and $\tau = T_{io}/T_B$ where $T_{io}$ is the free stream gas temperature. Thus

$$I_e = \frac{2\pi n_e}{(2\pi R T_B)^{3/2}} \int_o^\infty (R T_{io})^2 \tilde{v}_r^3 \exp\left(-\frac{\tau}{2} \tilde{v}_r^2\right) d\tilde{v}_r$$

Setting $z = \tilde{v}_r^2$, then

$$\int_o^\infty \tilde{v}_r^3 \exp\left(-\frac{\tau}{2} \tilde{v}_r^2\right) d\tilde{v}_r = \frac{1}{2} \int_o^\infty z \exp\left(-\frac{\tau}{2} z\right) dz$$

$$= \frac{1}{2} \left[ \frac{e^{-\frac{\tau}{2} z}}{(\tau/2)^2} \left(-\frac{\tau}{2} z - 1\right) \right]_{z=0}^{\infty} = \frac{2}{\tau^2}$$

Using this result, $I_e$ (flux emitted from the sphere) can be written as

$$I_e = \frac{8\pi n_e (R T_o)^2}{(2\pi R T_B)^{3/2}} \frac{1}{\tau^2} = 2 n_e \left(\frac{R T_o}{2\pi\tau}\right)^{1/2} \tag{42}$$

To obtain the flux $I_i$ (number of incoming molecules per unit time per unit area), let $u_o$ be the free stream velocity relative to the body and let $\theta$ be the angle between the velocity vector $u_o$ and the normal to the surface. (See diagram just below)

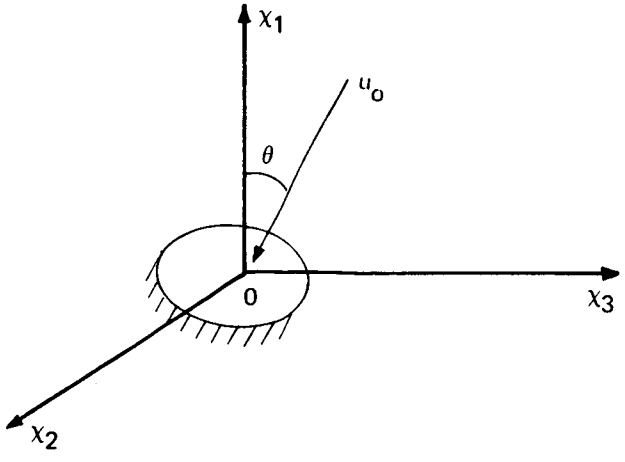

$$I_i = \int v_i \, dn_i = \int_{-\infty}^{\infty} \int_{-\infty}^{\infty} \int_{-\infty}^{o} n_i \, v_i \, f_i(v_i) \, dv_1 \, dv_2 \, dv_3 \tag{43}$$

where

$$f_i(v) = \frac{1}{(2\pi R T_o)^{3/2}} \exp \left\{ -(v_i - u_o)^2 \right\}$$

and

$$(v_i - u_o)^2 = (v_1 + u_0 \cos\theta)^2 + (v_2 + u_0 \sin\theta \cos\phi)^2 + (v_3 + u_0 \sin\theta \sin\phi)^2$$

Substitution leads to

$$I_i = \frac{n_i (R T_o)^2}{(2\pi R T_o)^{3/2}} \int_{-\infty}^{\infty} d\tilde{v}_3 \int_{-\infty}^{\infty} d\tilde{v}_2 \int_{-\infty}^{\infty} d\tilde{v}_1 \, \tilde{v}_1 \exp \left\{ -\frac{1}{2} \left[ (\tilde{v}_1 + u_0 \cos\theta)^2 + \right. \right.$$

$$\left. \left. (\tilde{v}_2 + \tilde{u}_0 \sin\theta \cos\phi)^2 + (\tilde{v}_3 + \tilde{u}_0 \sin\theta \sin\phi)^2 \right] \right\} \tag{44}$$

The integrations involved can be simplified by introducing new variables. In case of the $\tilde{v}_1$ - integration, let

$$y = (\tilde{v}_1 + u_0 \cos\theta)/\sqrt{2}$$

then

$$P_1 = \int_{-\infty}^{o} \tilde{v}_1 \exp \left\{ -\frac{1}{2} (\tilde{v}_1 + \tilde{u}_0 \cos\theta) \right\} d\tilde{v}_1$$

$$= \int_{-\infty}^{(\tilde{u}_0 \cos\theta)/\sqrt{2}} (\sqrt{2}\, y - \tilde{u}_0 \cos\theta) \exp \{ -y^2 \} \sqrt{2} \, dy$$

$$= 2 \int_{-\infty}^{(\tilde{u}_0 \cos\theta)/\sqrt{2}} y \exp \{ -y^2 \} \, dy - \sqrt{2}\, \tilde{u}_0 \cos\theta \int_{-\infty}^{(\tilde{u}_0 \cos\theta)/\sqrt{2}} \exp \{ -y^2 \} \, dy$$

$$= -\exp \left\{ \frac{-1}{2} \tilde{u}_0^2 \cos^2\theta \right\} - \sqrt{2}\, \tilde{u}_0 \cos\theta \cdot P_{11}$$

where

$$P_{11} = \int_{-\infty}^{(\tilde{u}_o \cos\theta/\sqrt{2}} e^{-y^2}\, dy$$

$$= \int_{-\infty}^{o} e^{-y^2}\, dy + \int_{o}^{\frac{\tilde{u}_o \cos\theta}{\sqrt{2}}} d^{-y^2}\, dy = \frac{\sqrt{\pi}}{2} + \frac{\sqrt{\pi}}{2} \text{erf} \left\{ \frac{\tilde{u}_o \cos\theta}{\sqrt{2}} \right\}$$

Hence

$$P_1 = -e^{-1/2\, \tilde{u}_o^2 \cos^2\theta} - \left(\frac{\pi}{2}\right)^{1/2} \tilde{u}_o \cos\theta \left[ 1 + \text{erf} \left\{ \frac{\tilde{u}_o \cos\theta}{\sqrt{2}} \right\} \right]$$

For the $v_2$- and $v_3$- integrations, introduce

$$y = (\tilde{v}_2 + \tilde{u}_o \sin\theta \cos\phi)/\sqrt{2}$$

and

$$z = (\tilde{v}_3 + \tilde{u}_o \sin\theta \sin\phi)/\sqrt{2}$$

$$P_2 = \int_{-\infty}^{\infty} e^{-1/2 (\tilde{v}_2 + \tilde{u}_o \sin\theta \cos\phi)^2} dv_2 = \int_{-\infty}^{\infty} \sqrt{2}\, e^{-y^2} dy = \sqrt{2\pi}$$

$$P_3 = \int_{-\infty}^{\infty} e^{-1/2 (\tilde{v}_3 + \tilde{u}_o \sin\theta \sin\varphi)^2} dv_3 = \int_{-\infty}^{\infty} \sqrt{2}\, e^{-z^2} dz = \sqrt{2\pi}$$

Using these results, $I_i$ (the incoming flux) can be written as

$$I_i = \frac{n_i (R T_o)^2}{(2\pi R T_o)^{3/2}} P_1 P_2 P_3$$

or

$$I_i = -\frac{n_i (R T_o)^2}{(2\pi R T_o)^{3/2}} 2\pi \left\{ e^{-1/2 \tilde{u}_o^2 \cos^2\theta} + \left(\frac{\pi}{2}\right)^{1/2} \tilde{u}_o \cos\theta \left[ 1 + \text{erf} \left( \frac{\tilde{u}_o \cos\theta}{\sqrt{2}} \right) \right] \right\}$$

$$= -n_i \left(\frac{R T_o}{2\pi}\right)^{1/2} \left\{ e^{-1/2\, \tilde{u}_o^2 \cos^2\theta} + \left(\frac{\pi}{2}\right)^{1/2} \tilde{u}_o \cos\theta \left[ 1 + \text{erf} \left( \frac{\tilde{u}_o \cos\theta}{\sqrt{2}} \right) \right] \right\} \quad (45)$$

The number of molecules reflected (or emitted) is equal to the number of molecules incoming, i.e. $I_e = I_i$. From eqs. (42) and (45), we obtain

$$\frac{n_e}{n_i} = \tau^{-1/2} \left\{ e^{-1/2\, u_o^2 \cos^2\theta} + \left(\frac{\pi}{2}\right)^{1/2} \tilde{u}_o \cos\theta \left[ 1 + \mathrm{erf}\left( \frac{\tilde{u}_o \cos\theta}{\sqrt{2}} \right) \right] \right\} \qquad (46)$$

In the hypersonic limit, i.e., $\tilde{v}_0$ becomes very large, except for $\theta = \pi/2$, Eq. (46) can be approximated by

$$\frac{n_e}{n_i} = 2 \left( \frac{\pi}{2} \right)^{1/2} \tau^{-1/2} \tilde{u}_o \cos\theta \qquad (47)$$

(e.g.) At $\theta = 70^0$ for $\tilde{u}_o = 10$ the difference between (46) and the hypersonic limit (47) is less than 0.5%.

# APPENDIX I

## PART D

## CYLINDRICAL GEOMETRY

This section presents a short discussion of the perturbation procedure applied to the problem of an infinitely long cylinder whose long axis is oriented transversely to the free-stream flow direction. The general theory is identical to that used for the spherical case. Also, similar geometrical approximations are invoked. As in the spherical case, the source radius is small compared to the observer distance, which in turn is small compared to the average mean free path.

There is a large degree of overlap of the present problem with the spherical geometry. The fundamental difference between the cylindrical geometry and the spherical geometry is that the cylindrical geometry gives rise to a stricter two-dimensional problem. In this problem the macroscopic flow variables depend on the r and $\theta$ cylinder coordinates. The Z direction is along the axis of the infinite cylinder; no variation can occur in this direction.

It can easily be shown that the total flux contributed to a point P some normal distance r from the body surface is a finite quantity when the flux arises from particles coming from a strip on the cylinder surface of width a $d\theta$ and infinite length. (The quantity a is the radius of the cylinder.) This establishes the validity of a two-dimensional geometry.

The integration of the linearized kinetic equation in the free-molecule flow approximation gives rise to the lowest-order approximation (beyond equilibrium) to the distribution function; namely,

$$\tilde{g}_o = \tau^2 \frac{\tilde{u}_0 \, a \, (1 + \cos 0)}{4\pi r v_r} (\theta - \theta') e^{-\frac{\tau v^2}{2}} \qquad (48)$$

where the meanings of the various parameters are equivalent to the spherical problem with the exception of the configurational coordinates. The zero-order (free-molecule) moments are straightforward integrations over the velocity coordinates.

The next-order approximation to the distribution function involves integration in configuration space. The integrand has the same form, in terms of the zero-order moments, as that for the spherical case. As a result of this integration, a logarithmic dependence upon the radial coordinate is obtained. This result is wholly expected and is known to be due to the infinite extent of the cylinder.

The range of integration is, in general, over the radial coordinate from infinity to the radius of the observation point. An approximation is employed in changing the lower limit from infinity to nL where n is a number of order unity and L is the average mean free path. This approximation can be used because the contribution to the integration from distances beyond 2 or 3 mean free paths is negligible. In effect the radial dependence of the second order approximation to the distribution function is given as $a/L \ln (r/L)$ for $r << L$.

In the numerical evaluation of the second-order correction to the radial number flux vector the form is the same as given in Equation (32) of this appendix. However, the detailed calculations are somewhat more lengthy than for the spherical case. The results for the cylinder case are presented in the main body of this report.